Measurement of Sylvian Fissure asymmetry and occipital bending in humans and Pan troglodytes

Accepted Manuscript

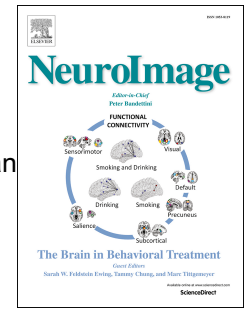

Measurement of Sylvian Fissure asymmetry and occipital bending in humans and Pan troglodytes

Lewis Hou, Li Xiang, Timothy Crow, François Leroy, Denis Rivière, Jean- François Mangin, Neil Roberts

PII: S1053-8119(18)30743-2

DOI: 10.1016/j.neuroimage.2018.08.045

Reference: YNIMG 15206

To appear in: *NeuroImage*

Received Date: 10 September 2017

Revised Date: 15 August 2018

Accepted Date: 17 August 2018

Please cite this article as: Hou, L., Xiang, L., Crow, T., Leroy, Franç., Rivière, D., Mangin, Jean-.Franç., Roberts, N., Measurement of Sylvian Fissure asymmetry and occipital bending in humans and Pan troglodytes, *NeuroImage* (2018), doi: 10.1016/j.neuroimage.2018.08.045.

Lewis Hou, Edinburgh Imaging, School of Clinical Sciences, University of Edinburgh, Edinburgh, EH16 4TJ, United Kingdom
lewis@scienceceilidh.com

Li Xiang, Edinburgh Imaging, School of Clinical Sciences, University of Edinburgh, Edinburgh, EH16 4TJ, United Kingdom
lxlxlx82@hotmail.com

Timothy Crow, Department of Psychiatry, Warneford Hospital, Oxford, OX3 7JX, United Kingdom
timjohncrow@gmail.com

François Leroy, Neurospin, Cognitive Neuroimaging Unit, INSERM, CEA, Paris-Saclay University, Gif-sur-Yvette, France
francois.leroy@cea.fr

Denis Rivière, Neurospin, INSERM, CEA, Paris-Saclay University, Gif-sur-Yvette, France
denis.riviere@cea.fr

Jean- François Mangin, Neurospin, INSERM, CEA, Paris-Saclay University, Gif-sur-Yvette, France
jmangin@gmail.com

[+]Neil Roberts, Edinburgh Imaging, School of Clinical Sciences, University of Edinburgh, Edinburgh, EH16 4TJ, United Kingdom
neil.roberts@ed.ac.uk

[+]Corresponding author

Measurement of Sylvian Fissure Asymmetry and Occipital Bending in Humans and Pan troglodytes

Abstract

The evolution of human-specific lateralised functions such as language has been linked to the development of structural asymmetries in the brain. Here we applied state of the art image analysis techniques to measure Sylvian Fissure (SF) asymmetry and Occipital Bending (OB) in 3D Magnetic Resonance (MR) images of the brain obtained in-vivo for 27 humans and 29 chimpanzees (Pan troglodytes).

SF morphology differed between species, with the human SF terminating more superiorly in right inferior parietal lobe, an asymmetry that was on average absent in chimpanzees (F (1,52) = 10.692, p = 0.002). Irrespective of morphology, Total SF Length was, as previously reported, leftward in humans but not in chimpanzees, although the difference did not reach significance between species. However, when only brains possessing comparable bilateral SF bifurcation morphology were compared, humans showed previously reported left-lateralised Anterior-Horizontal (AH-SF) and right-lateralised Vertical (V-SF) SF asymmetries. In contrast, chimpanzees lacked both asymmetries, and this approached significant difference between-species in the AH-SF segment (F (1, 34) = 2.365, p = 0.059).

On average in humans the left occipital lobe crossed the midline toward the right (Rightward OB) which was significantly different from the chimpanzee cohort that showed no average OB (Independent-Samples Mann-Whitney U Test, p = 0.012). Furthermore, OB was related to SF asymmetry in humans, such that the more rightward V-SF and leftward AH-SF, the more rightward the OB. This pattern of SF and OB asymmetries was found in 41.7% of human individuals with bilateral SF bifurcation but none of the chimpanzees.

To our knowledge, this is the first study highlighting that a pattern of SF and OB asymmetry distinguishes the human from the chimpanzee brain, and suggests this may be associated with a unique trajectory of brain development and functional abilities in humans.

Introduction

When Paul Broca first discovered the asymmetric role of the left hemisphere in language over a century ago, he suggested that humans were "... of all the animals, the one whose brain in the normal state is the most asymmetrical" (Broca, 1877; translated in Harrington (1987, p65 – 66). This began the long-standing hypothesis that cerebral asymmetry played an important role in human evolution which can now be investigated through advances in image analysis techniques for studying the structure of the brain using MRI.

The human brain was identified as globally asymmetric early on, with gross differences between left and right sides (Leuret and Gratiolet, 1839). In particular, the cerebral hemispheres have been reported to extend more posteriorly on the left and more anteriorly on the right (Petalia; Balzeau and Gilissen, 2010; Toga and Thompson, 2003) forming a counter-clockwise rotation of the human brain (the so-called Yakovlevian Torque after Yakovlev and Rakic (1966)). Being particularly pronounced in the posterior aspect (Myslobodsky et al., 1991), the left occipital pole often crosses the midline, a phenomenon referred to as Occipital Bending (OB; Glicksohn and Myslobodsky, 1993; Maller et al. 2014). Although its functional significance is still not known, the torque is evident early in brain development (Rajagopalan et al., 2011) and measures of it, including OB, are also disturbed in neurodevelopmental disorders including bipolar (Mackay et al. 2010; Maller et al., 2015), depression (Maller et al., 2014) and schizophrenia (Deutsch et al., 2000; Zhao et al., 2009; Maller et al., 2016; though see Narr et al, 2007). With regard to the latter, Crow (1999) has proposed an influential hypothesis that disturbance of the mechanisms that determine the development of usual human brain asymmetry may be of fundamental significance in causing psychiatric disorders such as schizophrenia.

One of the earliest prominent local asymmetries identified in the human brain was recognition that the Sylvian Fissures (SF) is longer in the left than the right hemisphere (Eberstaller, 1890) and also terminates higher in the right hemisphere (Cunningham, 1892). More recent research suggests SF asymmetry is also one of the earliest brain asymmetries to form during brain development, being visible from 20 gestational weeks (Habas et al. 2012). The SF can be divided into two components, anatomically split by the posterior bifurcation point ((B), Figure 1) with different asymmetries and potentially different associated functions, and which can be measured separately (Witelson and Kigar, 1992).

The Anterior-Horizontal SF (AH-SF) segment has frequently been reported to be longer in the left hemisphere (Figure 1) and contains the Planum Temporale (PT, Shapleske et al., 1999; Horn et al., 2009), Heschl's Gyrus (Shergill et al., 2000; Dorsaint-Pierre, 2006), and underlying Arcuate Fasciculus white matter tract (Takao et al., 2011) which are all left-lateralised. However, the relationship between structural and functional brain asymmetry is not simple (see Dorsaint-Pierre, 2006; Keller et al., 2011), the region is associated with language comprehension and production (Boeckx and Benítez-Burraco, 2014) and auditory processing (e.g. Johnsrude et al., 1997).

Posteriorly, the SF bifurcates in the inferior parietal lobe with the Vertical SF (V-SF) segment (the Posterior Ascending Ramus, Figure 1) reported to be longer, and terminate more superiorly, in the right hemisphere (Rubens et al., 1976; Witelson and Kigar, 1992). Associated with the Planum Parietale (PP, Jäncke et al., 1994), underlying Superior Longitudinal Fasciculus (SLF) and an adjacent deeper Superior Temporal Sulcus (Glasel et al., 2011; Leroy et al., 2015) that are all right-lateralised, the region is suggested to support networks involved in gesture, social cognition (e.g. Carter and Huettel, 2013), theory of mind and attentional processing (as part of the Temporal Parietal Junction, e.g. Saxe and Kanwisher, 2003; Samson et al., 2004; Santiesteban et al., 2012).

Taken together the SF and OB exhibit a directional asymmetry that is present in up to two thirds of the human population (Previc, 1991; Corballis, 2014). However, the evolutionary significance of this Typical brain asymmetry (e.g. LeMay, 1976; Toga and Thompson, 2003; Boeckx and Benítez-Burraco, 2014) remains to be determined.

One tool for better understanding the significance of laterality in human brain evolution is to compare homologous brain structures in other primates. Chimpanzees (*Pan troglodytes)* and humans diverged as late as 6.3 million years ago (Patterson et al., 2006) and despite the chimpanzee brain being about one third of the size of the human brain, share similarities in gross and sulcal anatomy. Several studies have found evidence of cerebral asymmetries in the chimpanzee, albeit often diminished compared to humans, including left lateralised Total SF Length asymmetry (Yeni-Komshian and Benson, 1976; Hopkins et al. 2000, Cantalupo et al. 2003), SF depth asymmetry (Bogart et al. 2012), leftward PT surface area asymmetry (Gannon et al., 1998; Hopkins et al., 2016), and rightward PP surface area asymmetry (Gannon et al. 2005; Taglialatela et al. 2007) (see Hopkins et al. 2015 for a review).

A limitation of previous comparative studies of the SF is that they do not measure chimpanzee AH-SF and V-SF separately, perhaps as the posterior bifurcation point (a unique feature among Great Apes (*Hominidae*, Gannon et al., 2001)) is often missing (up to 24%, Taglialatela et al., 2007). Consequently, it is challenging to make direct comparisons from previous results of SF asymmetry in humans and chimpanzees.

Furthermore, the morphology of the chimpanzee SF has been documented to be distinct from humans, with a more anterior orientation and lower termination (Inverted Type, Ide et al., 1996; Taglialatela et al, 2007) in inferior parietal lobe. This region has undergone considerable expansion (Coolidge, 2014) and cytoarchitectural re-organisation in humans (Buxhoeveden et al., 2001; Caspers et al., 2011; Binkofski, Klann and Caspers, 2016) and SF morphology and asymmetry may be measurable correlates of evolutionary differences between the human and chimpanzee brain.

There are relatively few studies of the global asymmetry of the chimpanzee brain and whether or not it possesses a Torque. Endocast studies suggest two-thirds of chimpanzees have human-like leftward occipital petalia (Balzeau and Gilissen, 2010; Balzeau et al., 2012) though there are many limitations to endocast methods (Falk, 1980). OB, as the posterior aspect of the torque, can be objectively measured using automatic brain imaging techniques and to our knowledge has never been measured in chimpanzees, despite evidence for reorganisation of the occipital lobes having occurred during evolution (Holloway, 2015).

The present study is the first to measure SF asymmetry (both morphology and length) and OB in humans and chimpanzees and uses advanced image-processing tools available in Freesurfer (Dale et al., 1999; freesurfer.net), FSL (Smith et al., 2004; fsl.fmrib.ox.ac.uk) and BrainVISA (Fischer et al., 2012; brainvisa.info) software. Measuring SF asymmetry and OB will determine if there is also a joint asymmetry of these components in chimpanzees. This analysis can potentially inform on whether OB and SF asymmetries evolved together (i.e. concerted evolution) or independently (i.e. mosaic evolution) (Reyes and Sherwood, 2015) and secondly, whether the asymmetries emerged before the divergence of humans as a conserved trait, or developed uniquely in humans.

We hypothesise that the majority of humans show a default pattern of lateralised SF asymmetry that is related to rightward OB, both of which are lacking in chimpanzees.

Specifically we seek to obtain answers to the following 4 questions:

1. Does population-level SF morphology asymmetry (including positional asymmetry of SF landmarks and bifurcation morphology) exist in humans and chimpanzees?

2. Does population-level SF length asymmetry (particularly of AH-SF and V-SF components)

exist in humans and chimpanzees?

3. Do humans and chimpanzees have population-level OB?

4. Are SF and OB asymmetry related in either or both species?

METHODS

2.1 Subjects

3D Magnetic Resonance (MR) Images were obtained for 30 human subjects (13 males, 17 females) and 30 chimpanzees (14 males, 16 females; Table 1). The MRI scans for humans were acquired at the Magnetic Resonance and Image Analysis Research Centre (MARIARC), University of Liverpool, and for chimpanzees at the Yerkes National Primate Centre (YNPRC) in Atlanta, Georgia.

2.2 Image Analysis Methods

2.2.1 Imaging protocol

The scanning protocols have been described previously (Keller et al., 2009). Briefly, humans and chimpanzees were scanned using a T1-weighted magnetization-prepared rapid-acquisition gradient echo (MPRAGE) protocol using a Siemens 3 tesla Trio MR system (Siemens Medical Systems, Erlangen, Germany). The acquisition parameters were TR 2300 ms, TE = 4.4 ms, TI 1100 ms, flip angle = 8°, FOV = 200 mm x 200 mm). In plane resolution was 0.6 mm x 0.6 mm for both cohorts and slice thickness was 1.0 for humans and 0.6 mm for chimpanzees, respectively. Acquisition time for human and chimpanzees subjects was 12 minutes, and 36 minutes, respectively. Comparable between-tissue contrast was present in the scans for both cohorts. The scanning had local Research Ethics Committee (REC) approval and all human participants provided written consent. The chimpanzee scanning followed YNPRC standard procedure, with subjects first being immobilised through ketamine injections (10mg/kg) and anesthetized with propofol (40-60 mg. kg^{-1}. h^{-1}). Subjects were transported from and back to their home environment and imaging facilities (total time ~ 2 hours) and scanned whilst remaining anesthetized. Scanning was conducted with the chimpanzee's head placed in a human head-coil in the supine position. The archived MRI data were uploaded onto a computer for pre-processing and analysis.

2.2.2 Image Preprocessing and Sulcal Extraction

Oil-capsules placed on the left side of the head during scanning were manually inspected to unequivocally confirm lateral direction prior to skull-stripping using FSL. All human and chimpanzee 3D MR images were transformed to the standard space of the MNI atlas (Mazziotta et al. 2001) in FSL (FMRIB Software Library Version 5.0) using a 7 DOF linear registration (3 rotation, 3 translocation and 1 uniform scaling). The 7 DoF registration is particularly important to enable the chimpanzee brains to be successfully processed using the FreeSurfer pipeline designed for human brains. This registration does not alter the morphological shape of the cerebral surface and the uniform scaling factor that is output is recorded as it allows computation of the size of sulci in the real world. Subsequently all images were processed using the standard Freesurfer (Version 5.3.0) pipeline running on a desktop computer (Mac OSX version 10.9.5) to obtain high quality reconstructions of the surface of the brain in native space, and which are used in the subsequent analyses of the Sylvian Fissure and occipital bending. It is to be noted that the output of the 7 DOF registration, and whether an asymmetric or symmetrized template is used, is not relevant for processing using the FreeSurfer pipeline which simply requires knowledge of the orientation (i.e. which way is up and which side is left and right) of the brain and for the chimpanzee brain to have been scaled to be approximately the same size as the human brain. More details are provided in Hopkins et al. (2017). Three human scans and

two chimpanzee scans of the original scans did not meet quality control requirements and were not successfully processed through this stage. The resulting brain segmentations and masks were imported into BrainVISA's Morphologist Pipeline 2012 (Version 4.4.4) to generate and automatically label 3D sulcal graph folds. The SF labels were visually checked and manually corrected using BrainVISA's visualisation software Anatomist. These steps are demonstrated in Figure 2.

2.3 Sylvian Fissure Morphology and Processing

2.3.1 Sylvian Fissure Anatomy

Human and chimpanzee MR images were inspected using BrainVISA software to identify the key SF landmarks in 3D (Figure 1) the Anterior Bifurcation Point (A), the Termination Point of the PAR (S_1) and, when present, the Posterior Bifurcation Point (B). In particular, (A) is determined as the point where the anterior ascending ramus and anterior horizontal ramus join the SF (Ono et al 1990), (S_1) is the posterior limit of the SF and (B) is the point where the SF may branch into the PAR and PDR. Furthermore, (B) splits the SF into an Anterior-Horizontal SF segment (AH-SF) (i.e. from landmarks A to B, Figure 1) and the PAR forms the Posterior Vertical SF segment (V-SF) (i.e. from landmarks B to S_1, Figure 1). PDR orientation was used to determine Bifurcation Types (see below), but as in Witelson and Kigar (1992), the length of the PDR was not measured.

2.3.2 Sylvian Fissure Sulcal Mesh Processing

All scans were checked to ensure that each landmark was correctly identified by the software so as to enable the accurate labelling and measurement of both the AH-SF and V-SF aspects if present. Landmark (B) was often missed by the software, and therefore was manually identified and used to split the SF sulcal fold accordingly. In particular, a method was developed using the Anatomist Software tool kits cross-referencing landmark (B) at three different sagittal depths to ensure 3D morphology was respected. The SplitFold tool was used to cut the SF mesh surface along the line joining these three landmarks so as to generate two separate 3D meshes corresponding to the V-SF and AH-SF (Figure 3).

2.4 Whole Cohort Analysis of Discrete Variables

2.4.1 Length Measurements of SF

The lengths of the relevant sulcal meshes were automatically obtained using the Morphometric's Toolkit in BrainVISA. Total SF Length was measured from (A) to (S_1) for the Whole Cohort (Witelson and Kigar, 1992; Figure 1). An Asymmetry Index (AI) was computed for Total SF Length, using the formula ((R-L)/((L+R)*0.5)) where R and L refer to the corresponding coordinates in the right and left hemisphere respectively (Eidelberg and Galaburda, 1982; Steinmetz et al., (1990)). Following previous comparative research conventions, if AI was +0.025 or higher, SF length asymmetry is classified as rightward, if AI was -0.025 or lower SF length asymmetry is classified as leftward, and if AI was between these two values SF lengths were classified as symmetrical (e.g. Cantalupo, Pilcher and Hopkins, 2003).

2.4.2 Positional Asymmetries

The 3D co-ordinates of the beginning (A) and end (S_1) of the SF in the superior-inferior and anterior-posterior directions were recorded for each cerebral hemisphere (Figure 1). A corresponding AI was computed by applying the same formula as above to these coordinate values. For each landmark, if AI was +0.025 or higher, the landmark is classified as being more superior or anterior on the right, if AI was -0.025 or lower, the landmark is classified as being more superior or anterior on the left, and if AI was between these two values, the landmark is classified as symmetrical.

2.4.3 Discrete OB Analysis

For directional analysis of OB, a threshold of 3 degrees was used to classify OB as either left, right, or symmetrical.

2.5 Analysis of Hemispheres with Bifurcation

2.5.1 Bifurcation Types

For each cerebral hemisphere in which (B) was present a further classification was performed according to the method of Ide et al. (1996). Four sub-types were defined based on the conformation of the PAR (V-SF) and the PDR. Generally, both PAR and PDR were directed posteriorly and were defined as Superior, Inferior or Symmetrical Bifurcation Type based on whether PAR was longer, shorter or the same length as PDR, respectively. Occasionally, PAR was directed anteriorly and PDR posteriorly and this constitutes the fourth type, named the Inverted Bifurcation Type regardless of the respective lengths of PAR and PDR, as also defined by Ide et al. (1996, See Figure 4). Classification was performed based on inspection of a lateral view of the cerebral hemisphere sulcal mesh produced using BrainVISA. In some cerebral hemispheres the SF had no bifurcation point (Figure 4).

2.5.2 Bifurcation Point Positional Asymmetry

In hemispheres with a bifurcation, the 3D co-ordinates of the bifurcation point (B) in both superior-inferior and anterior-posterior directions were also recorded, and AI computed as described in Section 2.4.2 above.

2.6 Bilateral Bifurcation Cohort SF Length Measurements

Humans and chimpanzees in which (B) was present in both hemispheres form subsets referred to as the respective human and chimpanzee "Bilateral Bifurcation Cohort".

A separate analysis was performed of the lengths of AH-SF and V-SF and corresponding AI in the bilateral bifurcation cohort and differences between species were investigated. Based on previous research (Witelson and Kigar, 1992), a Typical SF pattern is defined as a left-lateralised AH-SF and right-lateralised V-SF in the same individual brain and the opposite conformation (rightward AH-SF and a leftward V-SF) being described as the "Reversed SF Pattern".

2.7 Occipital Bending

OB was measured automatically using a programme written in Matlab (Version R2011b) by XL. Using the skull-stripped, transformed and size normalized human and chimpanzee segmentations, a smooth outer surface tightly covering each hemisphere was generated for each cerebral hemisphere by tessellation on top of the smoothed brain volume that had been sulcus-filled using the morphologic closing operation. Because the low dimensional transformation is not sufficient to align the centre of the brain surface to the centre of MNI space (i.e. x=0), particularly when the brain was very asymmetric, the alignment of the brain surface is adjusted as follows: i) the mid-sagittal plane is estimated as the plane which best fits the medial surface of the brain lying within 5 mm of x=0 and ii) the angle α between the middle sagittal plane and x=0 was computed and the brain outer surface was rotated by this angle. Following the reorientation, surfaces were fitted to the vertices of the medial surface of the left and right cerebral hemisphere in the last quarter of the anterior-posterior length of the brain. The angle between the normal of these fitted planes and the normal of the MNI midsagittal plane was calculated for the left and right hemispheres. The OB measurement was computed as the average of the two values.

2.8 Statistical Analysis

For each species, one-way *t*-tests were used to determine whether AI was significantly asymmetric in either direction for Total SF Length and Trajectory in the Whole Cohort and additionally for AH-SF and V-SF length and positions in the Bilateral Bifurcation Cohort.

Between-species differences in SF length, Bifurcation position and OB were examined using one of two approaches. If the data fulfilled the criteria of equal homogeneity of variances for parametric tests, a MANCOVA analysis was performed with sex and age as a covariate. If the data were non-parametric an Independent-Samples Mann-Whitney U-Test was performed.

Population distribution differences in OB, Bifurcation Type, Bifurcation Trajectory and SF length were compared using Chi-squared analysis. Statistical analysis was conducted using SPSS Statistics (version 20.0; IBM, Armonk, NY).

To explore whether asymmetries were related, bivariate Pearson's correlations were computed between Total-SF length asymmetry, SF Trajectory asymmetry and OB in the Whole Cohort, and additionally between AH-SF and V-SF length asymmetry, positional asymmetry and OB in the Bilateral Bifurcation Cohort in both species separately. Differences between independent correlation coefficients of the different species were judged using Fisher Z transformation.

RESULTS

3.1 Descriptive Statistics

The 3D MRI brain images for 27 Humans and 28 Chimpanzees were successfully processed through FSL, Freesurfer and BrainVISA (91.7%). The sex ratio was not significantly different between humans (14 males, 13 females) and chimpanzee cohorts (12 males, 16 females). There was a difference between the average age (t (53) = 4.093, $p < 0.001$) (Table 1) between humans (range: 19 – 60 years) and chimpanzees (range: 6 – 43 years).

3.2 Analysis of SF Bifurcation Point Frequency

(A) and (S_1) SF landmarks were well-defined on all scans. (B) was present in 51/54 hemispheres in humans (94.4%) and 38/56 hemispheres in chimpanzees (67.9%) and the distribution difference between species is significant (χ^2 (3, n=88) = 48.6, p <0.001) (see Table 2). (B) was present bilaterally in 24 humans (89%) and 14 (50%) chimpanzees (*Bilateral Bifurcation Cohort).*

All human cases of cerebral hemispheres missing the bifurcation point (B) (i.e. 3/54 which is 5.6% of total cohort) were on the left side. In chimpanzees, (B) was missing most often on the left (13/18, 72.2%) compared to the right hemisphere (5/18, 27.8%).

3.3 Analysis of SF Anatomy in the *Whole Cohort*

3.3.1 Total-SF Length Analysis

Total SF Length in the whole human cohort (*n*: 27) was significantly leftward asymmetric (t (26) = -2.184, p = 0.038; Mean AI: -0.062, SD: -0.147; Figure 5(ii), Figure 6) whereas in chimpanzees (*n*: 28) no significant asymmetry was observed (t (27) = 0.558, p = 0.582, *ns*; Mean AI: 0.019, SD: 0.178; Figure 5(ii), Figure 6). The difference between Total SF Length asymmetry showed a trend towards significance between the species (F (1, 52) = 3.435, p = 0.070, *ns*) (Figure 5(i), Figure 6).

In humans, leftward asymmetry of the Total SF Length was found to be most frequent (44.4%), followed by rightward asymmetry (33.3%) and no significant asymmetry (22.2%). Chimpanzees

did not differ significantly from humans in these frequencies, with both left and right having joint largest incidence (46.4%) and a small number showing no asymmetry (7.1%) (χ^2 *(2, n: 55) = 2.750*, $p = 0.253$, *ns*).

3.3.2 Sylvian Fissure Landmark Positional Analysis

In the Whole Cohort, the position of (A) was not significantly asymmetric in either Anterior-Posterior or Superior-Inferior directions for either species (Table 3). (S_1) was more anterior in the right than the left hemisphere in both humans and chimpanzees (Humans: t (26) = -4.674, $p < 0.001$; chimpanzees t (28) = -3.186, $p = 0.004$), and more superior on the right in humans (t (26) = - 2.752, $p = 0.011$, Mean: 0.0642, SD: 0.11) but not in chimpanzees (t (28) = -0.446, p = 0.659; Mean: 0.004, SD: 0.05) (Figure 7). The positional asymmetry of S_1 on the superior-inferior axis was highly significantly different between species (F (1,52) = 10.692, p = 0.002).

3.3.3 Whole Cohort Interaction with Age and Sex

Neither age (F (5, 44) = 1.012, $p = 0.422$, *ns*) nor sex (F (5,44) = 1.357, $p = 0.259$, *ns*) were significant co-variates with the measures of Total SF Length or the positional asymmetries of S_1 or A.

3.4 Analysis of SF Anatomy in All Hemispheres with Bifurcation

3.4.1 Bifurcation Type Analysis

Analysis of all hemispheres with bifurcated SF revealed that humans bifurcations were most commonly of Superior Type (74.5%), occurring slightly more in the right hemisphere (81.5% versus 59.3% in left hemisphere). Chimpanzees were most commonly of Inverted Type (83.3%) with V-SF pointing anteriorly, particularly in the right-hemisphere (74.1% compared to 37.0% in the left, Figure 3; Figure 7). The distribution of bifurcation types was statistically different between species (χ^2 (3, *n: 88*) = 48.06, $p < 0.001$) (see Table 2).

3.4.2 Bifurcation Point Positional Landmark Analysis

Where hemispheres had a SF bifurcation, (B) was significantly more anterior on the right SF compared to the left in humans (t (24) = -3.098, $p = 0.005$; Mean: 0.061, SD: 0.10), but not in chimpanzees (t (16) = -0.117, $p = 0.909$, *ns*; Mean: 0.001, SD: 0.04). The asymmetry in the Anterior-Posterior direction was statistically significant between species (F (1,40) = 5.716, $p = 0.022$). There was no significant asymmetry of the position of (B) in the Superior-Inferior direction in either species – i.e. (B) was not any more superior in either the left or the right cerebral hemisphere (Table 3, Figure 7).

3.5 Analysis of SF Anatomy in the Bilateral Bifurcation Cohort

3.5.1 AH-SF, V-SF and Total-SF Length Analysis

The human *Bilateral Bifurcation Cohort* (*n*: 24) showed the previously reported Typical SF pattern consisting of significantly leftward AH-SF (t (23) = -3.517, $p = 0.002$; Mean AI: -0.191, SD: 0.266) (Figure 5(iii)) and significantly rightward V-SF (t (23) = 2.869, $p = 0.009$; Mean AI +0.383, SD: 0.65) (Figure 5(iv)). Similar to the Whole Cohort analysis, Total SF Length was also not significantly asymmetric (t (23) = -1.874, $p = 0.074$, *ns*; AI: -0.058, SD: 0.152) (Table 4, Figure 6(ii) in the Human Bilateral Bifurcation Cohort).

For the chimpanzee *Bilateral Bifurcation Cohort* (*n*: 14) there were no asymmetries in either AH-SF (t (13) = -0.027, $p = 0.979$, *ns*, Mean AI: -0.017, SD: 0.198)(Figure 5(iii)), V-SF (t (13) = 0.850, $p = 0.411$; Mean AI: +0.104, *ns*, SD: 0.54) (Figure 5(iv)) or Total-SF (t (13) = 0.420, $p = 0.682$, *ns*, AI: +0.001, SD: 0.155) length (Table 4, Figure 6ii).

AH-SF length asymmetry showed a trend towards statistical significance between species (F (1, 34)

= 2.365, p = 0.059, *ns*) and V-SF (F (1, 34) = 1.881, p = 0.179, *ns*) or Total-SF (F (1, 34) = 0.728, p = 0.399, *ns*) length asymmetries did not reach statistical difference (Table 4, Figure 6(ii)).

Analyses of patterns of AH-SF and V-SF within individual brains showed that of the humans with bilateral bifurcations, 15/24 (62.5%) had the Typical pattern of SF asymmetries whereas only 3/24 (12.5%) had the Reversed pattern. Only 5/14 of the chimpanzees with bilateral bifurcations had the Typical pattern (35.7%) and 3/14 (21.4%) had the reversed SF patterns. The remaining subjects (6/14) showed a mixed phenotype, however, the difference in distributions between species did not reach statistical significance (χ^2 *(2, n: 38) = 2.545,* p = 0.280, *ns*; Figure 8).

3.5.2 Age and Sex in the Bilateral Bifurcation Cohort

The analysis of AH-SF, V-SF and Total SF with age (F (3, 32) = 0.278, p = 0.841, *ns*) and sex (F (3 32) = 0.486, p = 0.695, *ns*) as covariates alongside species found neither component significantly interacted with these measures.

3.6 Occipital Bending

3.6.1 Occipital Bending

OB could be measured in all but two of the scans (two chimpanzees) successfully processed by FSL, Freesurfer and BrainVISA. Humans showed significant rightward OB (t (26) = 2.889, p = 0.008; Mean: 3.38 degrees, SD: 6.08, *n*: 27) whereas chimpanzees had OB angles of small magnitudes and on average show no significant OB (t(26)= -0.039, p = 0.0969, *ns*; Mean OB: -0.266 degrees, SD: 3.53, *n*: 27) (Figure 5(i)). The difference between species in OB asymmetry is significant (Independent-Samples Mann-Whitney U Test, p = 0.012) suggesting that rightward OB is a specific characteristic of the human species.

3.6.2 Population Frequency

In humans, 48.1% (13/27) of scans showed rightward OB, 40.7% (11/27) symmetric OB and 11.1% (3/11) leftward OB using a threshold of 3 degrees in either rightward or leftward directions. In contrast, the majority of chimpanzees scans showed symmetric OB (66.7%, 18/27), with fewer brains showing leftward OB at 18.5% (or 5/27) and rightward OB (14.8%, or 4/27) (Figure 8). The distribution of the number of humans and chimpanzees in the different OB categories was highly significantly different between species (χ^2 *(2, n: 54) = 17.73,* p < 0.001).

3.6.3 OB, Age and Sex

When OB was analysed with age (F (1, 49) = 2.444, p = 0.124, *ns*) and sex (F (1, 49) = 0.078, p = 0.782, *ns*) as co-variates no significant effects were detected suggesting at least in this cohort, age and sex did not affect the OB.

3.7 SF and OB Interactions

3.7.1 *Co-occurrence Frequency*

In the Bilateral Bifurcation Cohorts, 10/24 (41.7%) of human had the Typical SF pattern co-occurring with rightward OB (default asymmetry; Figure 8), but none of the chimpanzee cohort had this combination on account of all of those with rightward OB missing (B) on the right side. This suggests there is a human-specific relationship between the Typical SF (leftward AH-SF and rightward V-SF) length asymmetries and rightward OB missing in chimpanzees.

3.7.2 Correlations

3.7.2.1 OB and SF Positional Measures

In the Whole Cohort, the more rightward the OB angle, the more superior and anterior the termination point (S_1) of the SF in the right relative to the left hemisphere (Superior-Inferior Axis AI: *r*: 0.428, $p = 0.001$, *n:* 53 ; Anterior-Posterior Axis AI *r*: -0.421, $p = 0.002$, *n:* 53).

In the human cohort there is a relationship between the position of S_1 and OB in both directions (AI on the Superior-Inferior Axis: *r*: 0.425, $p = 0.027$, *n*: 27, Figure 9(i); AI on the Anterior- Posterior Axis *r*: -0.423, $p = 0.028$, *n*: 27, Figure 9(iii)). Chimpanzees have the same relationship in the Anterior-Posterior (*r*: -0.542, $p = 0.004$, *n:* 26, Figure 9(iv)) but not Superior-Inferior axis (*r*: 0.179, $p = 0.381$, *ns*, *n*: 26, Figure (ii)) though the difference between species did not reach significance (Superior-Inferior Axis AI: $Z = 0.93$, $p = 0.352$, *ns*, two tailed; Anterior-Posterior Axis AI: $Z = 0.53$, $p = 0.60$, *ns*, two tailed).

3.7.2.2 OB, SF and Age

The relationship between OB, SF length measures and age were explored both in the Whole Cohort and in each species separately. Age did not correlate with any measure in the full cohort (*p* values ranging from $p = 0.348$ (Total SF AI) to $p = 0.862$ (Vertical SF) and with OB as *r*: -0.027, $p = 846$, *ns*, *n: 53*).

However, when both species were analysed separately, there was a significant correlation between OB and age in chimpanzees (*r: -0.547,* $p = 0.003$, *n: 27)* but not in humans (*r: -0.032,* $p = 0.878$, *n: 26)*, a difference which is significant between the species (*Z=-1.99, p = 0.0466, two tailed).* This suggests that the older the chimpanzee, the more leftward the OB angle.

3.7.2.3 OB and SF Length Measures

There was no relationship in the Whole Cohort between Total SF Length and OB, in either humans (*r*: -0.211, *p*: 0.291, *ns*, *n*: 27) or chimpanzees (*r*: -0.216, *p*: 0.289, *ns*, *n*: 26) (Z = 0.018, p = 0.986, *ns*, two tailed).

In only the Bilateral Bifurcation Cohort, where AH-SF and V-SF lengths are available, humans showed a relationship between AH-SF and OB (*r*: -0.599, *p*: 0.001, *n*: 27, Figure 9) though chimpanzees did not (*r*: -0.379, *p*: 0.056, *ns*, *n*: 26). Similarly, V-SF and OB were related in humans (*r*: +0.506, *p*: 0.012, *n*: 24) but not in chimpanzees (*r*: +0.142, *p*: 0.645, *ns*, *n*: 13) (Figure 9). These relationships suggest a human-specific interaction where the more rightward the OB angle, the more leftward the AH-SF and rightward the V-SF length asymmetry. However, the difference between-species correlations with OB were not significant for either AH-SF (Z = -0.74, p = 0.459, *ns*) or V-SF (Z = 1.078, p = 0.281, *ns*).

3.7.2.3 SF Length and Positional Measures

The positional asymmetry of the Superior-Inferior Axis of landmark S_1 is strongly correlated with the length asymmetry V-SF in the *Bilateral Bifurcation Cohort* (n = 38; r = 0.791, p < 0.001). This is especially the case in humans (r = 0.857, p < 0.001, *n:* 24) but also for the chimpanzees (r = 0.539, p = 0.047, *n:* 14) (Z = -1.825, p = 0.068, *ns*, two tailed). The reverse relationship is also true for the AH-SF, such that the longer the left segment, the more superior the SF terminates on the opposite hemisphere (e.g. right) (r = -0.452, p = 0.001, *n*: 54).

The positional asymmetry measures of the Superior-Inferior and Anterior-Posterior axes were not correlated in the whole sample (*r*: -0.118, p = 0.389, *ns*) or in either species (Humans: *r*: = 0.318, p = 0.106, *ns*; Chimpanzees: *r*: 0.082, p = 0.678, *ns*) suggesting that they are measuring independent components.

Discussion

SF Asymmetries (Morphology)

The first aim of the study was to measure the SF of humans and chimpanzees, and here we showed there are fundamental differences in both length and morphology between species. Human Total SF Length is longer on the left and terminates both more superiorly and more anteriorly on the right (Figure 5(ii), Figure 6(i)), matching findings from other methods including automated surface-based (Lyttelton et al., 2009; Xiang et al. 2018) and vertex-based sulcal pattern analysis (Csernansky et al., 2008) and dissection (Rubens et al., 1976). Chimpanzees, in contrast, have largely symmetrical Total SF Length, and a SF that terminates more anteriorly, but not more superiorly, on the right. One study found inconsistent asymmetries in the position of (B) in chimpanzees (LeMay and Geschwind, 1975). However, to our knowledge, the lack of an asymmetry in the chimpanzee brain corresponding to a more superior termination of the right SF, which is a characteristic feature of the human brain, is a novel finding.

SF bifurcation patterns are also distinctive in each species, with the human SF frequently bifurcating and being most often as the Superior Bifurcation Type. Chimpanzee SF bifurcate less frequently and when they do are most often of Inverted Bifurcation Type (Figure 4). Both findings are in line with previously reported frequencies of 92.8% of 152 human cerebral hemispheres (Jäncke et al., 1994) and 76% of 76 chimpanzee cerebral hemispheres (Taglialatela et al., 2007)).

SF Asymmetries (length)

When the SF is bifurcated bilaterally, humans show the Typical asymmetry pattern (i.e. leftward AH-SF and rightward V-SF length) as previously reported (Witelson and Kigar, 1992). This pattern is

found in just under two-thirds of individual brains (62.5%). In contrast, only 35.7% of chimpanzees in the equivalent bilateral bifurcation cohort had the Typical SF pattern, and neither AF-SF nor V-SF was lateralised in chimpanzees as a whole.

Although the results of the present study appear to contradict previous findings that chimpanzee SF length is asymmetric (e.g. Yeni-Komshian and Benson, 1976; Hopkins, Pilcher and MacGregor, 2000; Cantatupo, Pilcher and Hopkins, 2003; Bogarts et al., 2012), previous studies did not use the same anatomical landmarks or protocol to measure AH-SF and V-SF individually. The significant between-species differences measured in this study suggest that it will be of interest to continue to measure these components separately in future comparative research.

Ultimately, SF length asymmetry did not distinguish human and chimpanzee brains as clearly as positional morphology differences and past overreliance on length alone without considering morphology may account for previous conflicting findings.

OB Asymmetries

The second aim of the study was to measure OB. Zhao et al. (2009) developed a method to automatically analyse the interhemispheric fissure bending by computing the curvature features at each point of a fitted medial surface. However, this study did not provide a measurement in degrees of OB. We believe the present study is the first in which image analysis techniques have been used to automatically measure OB. According to our results, human brains have rightward OB on average (found in 48.1% of individuals), consistent with previous findings using manual single-slice methods (Maller et al., 2014, 2015) and study of the occipital component of the Torque (Thompson and Toga, 2003). Chimpanzees, however, show no significant OB on average (66.7% had no OB, and only 14.8% had rightward OB) and which, as far as we are aware, has never previously been reported. Although petalia imprints were found in 67% of chimpanzee endocasts (Balzeau et al., 2010; Balzeau et al. 2012), this suggests that OB, and particularly rightward lateralised, only developed in humans

Relationship between Asymmetries

Our final aim was to explore the relationship between SF asymmetries and OB. Human SF length, position and OB measures were correlated in the bilateral bifurcation cohort - such that the Typical SF pattern is associated with rightward OB - suggesting that they are related phenomenon in humans. This pattern was found in 41.7% of individual human brains with bilateral SF bifurcation. Furthermore, 86.7% of all rightward OB cases have leftward AH-SF and rightward V-SF, a prevalence very much higher than by chance. These findings are consistent with the report of a relationship between brain torque and leftward PT asymmetries in humans (Barrick et al. 2005).

In contrast, chimpanzees as a population did not show significant average OB, SF asymmetry, or correlation. Furthermore, no individual chimpanzee had the human Typical pattern of leftward AH-SF and rightward V-SF together with rightward OB (Figure 8). Together, these findings are consistent with the hypothesis of a human-specific Joint pattern of SF and OB asymmetry (Previs, 1991; Corballis, 2014).

Biological and Functional Implications of SF findings

There are many reasons why SF length and morphology may have developed to be asymmetric in humans. Structures within the SF are lateralised in humans, including the PT (e.g. Horn et al., 2009) and PP (e.g. Jäncke et al., 1994), but this has also been reported, albeit to a lesser extent, in chimpanzees too (e.g. Hopkins et al. 2016; Taglialatela et al., 2007). The inferior parietal lobe (IPL), which surrounds the posterior termination of the SF, has expanded considerably during human evolution to be uniquely large compared to other great apes (Rilling and Seligman, 2002; Coolidge,

2014). This has been accompanied by rearrangement of cytoarchitecture (Caspers et al., 2006, 2008; 2013) including region Tpt, the chimpanzee analogue of Wernickes Area (Spocter et al., 2010), and development of human-specific regions (e.g. PFm; Krubitzer, 2009; Caspers et al. 2011). Although laterality was not explicitly studied in these reports, the angular aspect of the human inferior parietal gyrus is reported to be larger on the right (Goldberg et al., 2013), raising the possibility that the higher termination and shortening in length of the right SF characteristic of the human brain may be a biomarker of an asymmetrically expanded IPL.

The observed differences in the structural asymmetry of the human and chimpanzee brain are particularly relevant within an evolutionary context as they potentially reflect regional functional reorganisation (Caspers et al., 2011; reviewed in Binkofski, Klann and Caspers, 2016) of networks involved in both language and motor planning/gesture in humans, through the left-lateralised Arcuate Fasciculus (AF, Rilling, 2014) and right-lateralised Superior Longitudinal Fasciculus (branch III, Hecht et al. 2015; Reyes and Sherwood, 2015; de Schotten et al., 2011) respectively. In parallel with our findings in the SF, the underlying white fiber tracts are reported not to be lateralised in chimpanzees (Rilling et al., 2008, Hecht et al., 2015), raising the possibility that surface asymmetries in humans may be related to lateralised white matter changes. Further research combining analysis of brain structural asymmetry with Diffusion Tensor Imaging (DTI) is needed to explore this suggestion, and already one study has found that AF asymmetry is correlated to surrounding grey matter asymmetry in humans (Takao et al., 2011).

Biological Implications: OB and Asymmetry Relationships

The biological significance of a generally rightward OB in the human brain which is absent in the chimpanzee brain is not clear, especially as the functional role of OB is still to be understood. Although a direct study of the functional significance of OB has yet to be performed, by using, for example, functional Magnetic Resonance Imaging (fMRI), the occipital lobes are known to be involved in visual processing and have reorganized throughout primate evolution (Holloway et al., 2003; de Sousa et al., 2010; Holloway, 2015). Rightward OB may be a consequence of human hemispheric specialization (Falk et al. 2014), brain scaling (Kaas, 2000; Kaas, 2006) or a spatial displacement of the hemispheres potentially driven by ventricular or subcortical asymmetries (Watkins et al. 2001; Maller et al., 2014, 2015; de Sousa et al., 2010). Our own findings support a link between SF and OB asymmetry, particularly as individual human brains with reversed SF asymmetry were also more likely to have reversed (i.e. leftward) OB.

Overall, humans exhibited a Joint pattern of SF and OB symmetry not found in chimpanzees, suggesting that SF asymmetry and OB are not independent from each other and reflect a concerted rather than mosaic evolution process (Reyes and Sherwood, 2015). Development may play a role in this connection, with both SF positional (Dubois et al., 2010; Habas et al. 2012) and occipital volume asymmetries (Rajagopalan et al., 2011; Tzarouchi et al., 2009) reported as early as 20 gestational weeks in humans, and continuing to develop from birth (LeMay, 1976, Chiron et al., 1997; Glasel et al., 2011) into adulthood (Sowell et al. 2002).

OB has yet to be studied during development of the human or chimpanzee brain, and detailed study of sulcal morphology in the young chimpanzee brain is also lacking and merits further investigation Gross brain development velocity already diverges from humans by 22 gestational weeks (Sakai et al., 2012) suggesting that future work looking into species differences in cerebral lateralisation should include study of brain development (see Gunz et al, 2012).

Limitations

The modest sample size is a limitation of this study, particularly as the low proportion of chimpanzees with bilateral bifurcations reduces the ability to measure the significance of AH-SF and V-SF asymmetry, and individual t-tests for asymmetry direction and correlational analyses were not corrected for multiple comparisons. This also prevented the independent consideration of sex

differences, with previous work suggesting that both the SF (Witelson and Kigar, 1992; Taglialatela et al., 2007) and OB asymmetries (Maller et al. 2014) exhibit sex differences (though see Narr et al. 2007). Sex was not a significant covariate in either SF or OB measures although a larger study is required to specifically address this point. Similarly, age has been shown to affect sulcal structure in humans (e.g. Sowell et al. 2012) and although age was also not a significant covariate in any of the analyses, we cannot definitively rule out an effect that was not detected in the cohorts with relatively modest size.

Lack of information on the handedness of the human participants is another limitation of the study, especially as this has been suggested to influence brain anatomy (e.g. Witelson & Kigar, 1992). However, effects may be particularly focused in motor areas (Amunts et al. 1997) and several larger, global studies have not found effects (e.g. Good et al. 2001, Narr et al. 2007).

Conclusions

In conclusion, the human and chimpanzee brain can be distinguished by clear differences in Sylvian Fissure (SF) morphology and Occipital Bending (OB) asymmetries. SF length also varies between the species, but requires careful attention to morphology to divide into two segments, AH-SF and V-SF, with respect to the bifurcation point. The human-specific higher termination of the SF on the right may be a structural correlate of human cerebral re-organisation in the IPL, with concomitant white matter connectivity and functional changes which should be explored more fully in future.

Furthermore, in humans, SF and OB asymmetries are significantly related to each other. They commonly form a Joint pattern that is clearly absent in the chimpanzee population and may arise early in brain development. Although further research needs to be done, this is both consistent with and builds on the hypothesis proposed over a century ago that structural asymmetries in the brain are associated with human's unique cognitive abilities.

REFERENCES

Amunts, K., Schlaug, G., Jäncke, L., Steinmetz, H., Schleicher, A., Dabringhaus, A. and Zilles, K. (1997). Motor cortex and hand motor skills: structural compliance in the human brain. *Human Brain Mapping*, *5*, 206–215.

Balzeau, A. and Gilissen, E. (2010). Endocranial shape asymmetries in Pan paniscus, Pan troglodytes and Gorilla gorilla assessed via skull based landmark analysis. *Journal of Human Evolution*, *59*, 54–69.

Balzeau, A., Gilissen, E. and Grimaud-Hervé, D. (2012). Shared Pattern of Endocranial Shape Asymmetries among Great Apes, Anatomically Modern Humans, and Fossil Hominins. *PLoS One*, *7*, e29581.

Barrick, T. R., Mackay, C.E., Prima, S., Maes, F., Vandermeulen, D., Crow, T.J. and Roberts, N. (2005). Automatic analysis of cerebral asymmetry: an exploratory study of the relationship between brain torque and planum temporale asymmetry. *NeuroImage*, *24*, 678–691.

Binkofski, F.C., Klann, J. and Caspers, S. (2015). On the Neuroanatomy and Functional Role of the Inferior Parietal Lobule and Intraparietal Sulcus. *Neurobiology of Language* (pp. 35–48). Elsevier Inc.

Boeckx, C. and Benítez-Burraco, A. (2014). The shape of the human language-ready brain. *Frontiers in Psychology, 5*, 1–23.

Bogart, S.L., Mangin, J.F., Schapiro, S.J., Reamer, L., Bennett, A.J., Pierre, P.J. and Hopkins, W.D. (2012). Cortical sulci asymmetries in chimpanzees and macaques: A new look at an old idea. *NeuroImage*, *61*, 533–541.

Buxhoeveden, D.R., Switala, A.E., Litaker, M., Roy, E. and Casanova, M.F. (2001). Lateralization of minicolumns in human planum temporale is absent in nonhuman primate cortex. *Brain, Behavior and Evolution*, *57*, 349–358.

Cantalupo, C., Pilcher, D.L. and Hopkins, W.D. (2003). Are planum temporale and Sylvian fissure asymmetries directly related? *Neuropsychologia*, *41*, 1975–1981.

Carter, R.M. and Huettel, S.A. (2013). A nexus model of the temporal–parietal junction. *Trends in Cognitive Sciences*, *17*, 328–336.

Caspers, S., Geyer, S., Schleicher, A., Mohlberg, H., Amunts, K. and Zilles, K. (2006). The human inferior parietal cortex: Cytoarchitectonic parcellation and interindividual variability. *NeuroImage*, *33*, 430–448.

Caspers, S., Eickhoff, S. B., Geyer, S., Scheperjans, F., Mohlberg, H., Zilles, K. and Amunts, K. (2008). The human inferior parietal lobule in stereotaxic space. *Brain Structure and Function*, *212*, 481–495.

Caspers, S., Eickhoff, S.B., Rick, T., Kapri, von, A., Kuhlen, T., Huang, R. et al. (2011). Probabilistic fibre tract analysis of cytoarchitectonically defined human inferior parietal lobule areas reveals similarities to macaques. *NeuroImage, 58, 362-380.*

Caspers, S., Schleicher, A., Bacha-Trams, M., Palomero-Gallagher, N., Amunts, K. and Zilles, K. (2013). Organization of the Human Inferior Parietal Lobule Based on Receptor Architectonics. *Cerebral Cortex*, *23*, 615–628.

Chiron, C., Jambaque, I., Nabbout, R., Lounes, R., Syrota, A. and Dulac, O. (1997). The right brain hemisphere is dominant in human infants. *Brain*, *120*, 1057-1065.

Coolidge, F.L. (2014) The exaptation of the parietal lobes in Homo sapiens. *Journal of Anthropological Sciences, 92,* 295–298.

Corballis, M. C. (2014). Left Brain, Right Brain: Facts and Fantasies. *PLoS Biology*, *12*, e1001767.

Crow, T.J. (1990). Temporal lobe asymmetries as the key to the etiology of schizophrenia. Schizophrenia Bulletin, 16, 433-443.

Csernansky, J. G., Gillespie, S. K., Dierker, D. L., Anticevic, A., Wang, L., Barch, D. M. and Van Essen, D. C. (2008). Symmetric abnormalities in sulcal patterning in schizophrenia. *NeuroImage*, *43*, 440–446.

Cunningham, D.J. (1892) *Contribution to the surface anatomy of the cerebral hemispheres*. Dublin: Royal Irish Academy.

Dale, A.M., Fischl, B. and Sereno, M.I. (1999). Cortical surface-based analysis I. Segmentation and surface reconstruction. *NeuroImage, 9*, 179-194.

de Sousa, A.A., Sherwood, C.C., Mohlberg, H., Amunts, K., Schleicher, A., MacLeod, C.E. et al. (2010). Hominid visual brain structure volumes and the position of the lunate sulcus. *Journal of Human Evolution*, *58*, 281–292.

Deutsch, C.K., Hobbs, K., Price, S.F. and Gordon-Vaugh, K. (2000). Skewing of the brain midline in schizophrenia. *Neuroreport*, *11*, 3985–3988.

Dorsaint-Pierre, R. (2006). Asymmetries of the planum temporale and Heschl's gyrus: relationship to language lateralization. *Brain*, *129*, 1164–1176.

Dubois, J., Benders, M., Lazeyras, F., Borradori-Tolsa, C., Leuchter, R.H-V., Mangin, J.F., and Hüppi, P.S. (2010). Strutural asymmetries of perisylvian regions in the preterm newborn. *NeuroImage*, *52*, 32-42.

Eberstaller, O. (1890). *Das Stirnhirn*. Wein and Leipzig: Urban and Schwarzenberg.

Eidelberg, D. and Galaburda, A.M. (1982). Symmetry and Asymmetry in the Human Posterior Thalamus Cytoarchitectonic Analysis in Normal Persons. *Archives of Neurology*, *39*, 325–332.

Falk, D. (1980). A reanalysis of the South African australopithecine natural endocasts. *American Journal of Physical Anthropology*, *53*, 525–539.

Falk, D. (2014). Evolution of the Primate Brain. In *Handbook of Paleoanthropology* (pp. 1495–1525). Berlin, Heidelberg: Springer Berlin Heidelberg.

Fischer, C., Operto, G., Laguitton, S., Perrot, M., Denghien, I., Rivière, D. and Mangin, J.F. (2012). Morphologist 2012: the new morphological pipeline of BrainVISA. In *Proceedings of the 18th HBM Scientific Meeting, Beijing, China. NeuroImage* (p. 670).

Gannon, P. J., Holloway, R. L., Broadfield, D. C. and Braun, A. R. (1998). Asymmetry of chimpanzee planum temporale: humanlike pattern of Wernicke's brain language area homolog. *Science*, *279*, 220–222.

Gannon, P.J., Kheck, N.M. and Hof, P.R. (2001). Language areas of the hominoid brain: a dynamic communicative shift on the upper east side planum. In: Falk, D., Gibson, K. R., *Evolutionary anatomy of the primate cerebral cortex*. Cambridge: Cambridge University Press.

Gannon, P.J., Kheck, N.M., Braun, A.R. and Holloway, R.L. (2005). Planum parietale of chimpanzees and orangutans: A comparative resonance of human-like planum temporale asymmetry. *The Anatomical Record Part A: Discoveries in Molecular, Cellular, and Evolutionary Biology*, *287A*, 1128–1141.

Glasel, H., Leroy, F., Dubois, J., Hertz-Pannier, L., Mangin, F. and Dehaene-Lambertz, G. (2011). A robust cerebral asymmetry in the infant brain: The rightward superior temporal sulcus. *NeuroImage*, *58*, 716–723.

Glicksohn, J. and Myslobodsky, M.S. (1993). The Representation of Patterns of Structural Brain Asymmetry in Normal Individuals. *Neuropsychologia*, *31*, 145–159.

Good, C.D., Johnsrude, I., Ashburner, J., Henson, R.N.A., Friston, K.J. and Frackowiak, R.S.J. (2001). Cerebral Asymmetry and the Effects of Sex and Handedness on Brain Structure: A Voxel-Based Morphometric Analysis of 465 Normal Adult Human Brains. *NeuroImage*, *14*, 685–700.

Gunz, P., Neubauer, S., Golovanova, L., Doronichev, V., Maureille, B. and Hublin, J. (2012). A uniquely modern human pattern of endocranial development. Insights from a new cranial reconstruction of the Neandertal newborn from Mezmaiskaya. Journal of Human Evolution. *Journal of Human Evolution*, *62*, 300–313.

Habas, P.A., Scott, J.A., Roosta, A., Rajagopalan, V., Kim, K., Rousseau, F. et al. (2011). Early Folding Patterns and Asymmetries of the Normal Human Brain Detected from in Utero MRI. *Cerebral Cortex*, *22*, 13–25.

Harrington, A. (1987). *Medicine, Mind, and the Double Brain*. Cambridge: Cambridge University Press.

Hecht, E.E., Gutman, D.A., Bradley, B.A., Preuss, T.M., and Stout, D. (2015). Virtual dissection and comparative connectivity of the superior longitudinal fasciculus in chimpanzees and humans. *NeuroImage*, *108*, 124-137.

Holloway, R.L., Broadfield, D.C., and Yuan, M.S. (2003). Morphology and histology of chimpanzee primary visual striate cortex indicate that brain reorganization predated brain expansion in early hominid evolution. *The Anatomical Record Part a: Discoveries in Molecular, Cellular, and Evolutionary Biology*, *273A*, 594–602.

Holloway, R.L. (2015). The Evolution of the Hominid Brain. *Handbook of Paleoanthropology*.

Hopkins, W.D., Pilcher, D.L. and MacGregor, L. (2000). Sylvian fissure asymmetries in nonhuman primates revisited: a comparative MRI study. *Brain, Behavior and Evolution*, *56*, 293–299.

Hopkins, W.D., Misiura, M., Pope, S.M. and Latash, E.M. (2015). Behavioral and brain asymmetries in primates: a preliminary evaluation of two evolutionary hypotheses. *Annals of the New York Academy of Sciences*, *1359,* 65-83.

Hopkins, W.D., Hopkins, A.M., Misiura, M., Latash, E.M., Mareno, M.C., Schapiro, S.J., and Phillips, K.A. (2016). Sex differences in the relationship between planum temporale asymmetry and corpus callosum morphology in chimpanzees (Pan troglodytes): A combined MRI and DTI analysis. *Neuropsychologia*, 93B, 325-334.

Hopkins, W.D., Li, X., Crow, T.J, Roberts, N. (2017). Vertex- and atlas-based comparisons in measures of cortical thickness, gyrification and white matter volume between humans and chimpanzees. *Brain Struct Function*, *222,* 229-245.

Horn, H., Federspiel, A., Wirth, M., Müller, T. J., Wiest, R., Wang, J. and Strik, W. (2009). Structural and metabolic changes in language areas linked to formal thought disorder. *The British Journal of Psychiatry, 194*, 130-138.

Ide, A., Rodríguez, E., Zaidel, E. and Aboitiz, F. (1996). Bifurcation patterns in the human sylvian fissure: hemispheric and sex differences. *Cerebral Cortex, 6*, 717–725.

Jäncke, L., Schlaug, G., Huang, Y. and Steinmetz, H. (1994). Asymmetry of the planum parietale. *Neuroreport*, *5*, 1161–1163.

Johnsrude, I.S., Zatorre, R.J., Milner, B.A. and Evans, A.C. (1997). Left-hemisphere specialization for the processing of acoustic transients. *NeuroReport*, *8*, 1761–1765.

Kaas, J.H. (2000). Why is brain size so important: Design problems and solutions as neocortex gets bigger or smaller. *Brain and Mind*, *1,* 7-23.

Kaas, J.H. (2006). Evolution of the neocortex. *Current Biology*, *16*, R910–R914.

Keller, S.S., Roberts, N., and Hopkins, W.D. (2009). A Comparative Magnetic Resonance Imaging Study of the Anatomy, Variability, and Asymmetry of Broca's Area in the Human and Chimpanzee Brain. *Journal of Neuroscience*, *29*, 14607–14616.

Keller, S.S., Roberts, N., Garcia-Finana, M., Mohammadi, S., Ringelstein, E.B., Knecht, S. and Deppe, M. (2011). Can the Language-dominant Hemisphere Be Predicted by Brain Anatomy? *Journal of Cognitive Neuroscience*, *23*, 2013–2029.

Krubitzer, L., 2009. In search of a unifying theory of complex brain evolution. *Annals of the New York Academy of Sciences, 1156,* 44–67.

LeMay, M. (1976). Morphological cerebral asymmetries of modern man, fossil man, and nonhuman primate. *Annals of the New York Academy of Sciences*, *280*, 349–366.

LeMay, M., and Geschwind, N. (1975). Hemispheric differences in the brains of great apes. *Brain, Behavior and Evolution*, *11*, 48–52.

Leroy, F., Cai, Q., Bogart, S. L., Dubois, J., Coulon, O., Monzalvo, K. et al. (2015). New human-specific brain

landmark: The depth asymmetry of superior temporal sulcus. *Proceedings of the National Academy of Sciences*, *112*, 1208–1213.

Leuret, F. and Gratiolet, P.-L. (1839). Anatomie comparée du système nerveux considéré dans ses rapports avec l'intelligence. Tome 1/par Fr. Leuret et P. Gratiolet... J.-B. Baillière (Paris).

Lyttelton, O.C., Karama, S., Ad-Dab'bagh, Y., Zatorre, R.J., Carbonell, F., Worsley, K. and Evans, A.C. (2009). Positional and surface area asymmetry of the human cerebral cortex. *NeuroImage*, *46*, 895–903.

Mackay, C.E., Roddick, E., Barrick, T.R., Lloyd, A.J., Roberts, N., Crow, T.J. et al. (2010). Sex dependence of brain size and shape in bipolar disorder: an exploratory study. *Bipolar Disorders*, *12*, 306–311.

Maller, J.J., Thomson, R.H.S., Rosenfeld, J.V., Anderson, R., Daskalakis, Z.J. and Fitzgerald, P.B. (2014). Occipital bending in depression. *Brain*, *137*, 1830–1837.

Maller, J.J., Anderson, R., Thomson, R.H., Rosenfeld, J.V., Daskalakis, Z. J. and Fitzgerald, P.B. (2015). Occipital bending (Yakovlevian torque) in bipolar depression. *Psychiatry Research: Neuroimaging*, *23,* 8-14.

Maller, J.J., Anderson, R.J., Thomson, R.H., Daskalakis, Z.J., Rosenfeld, J.V. and Fitzgerald, P.B. (2016). Occipital bending in schizophrenia. *Australian and New Zealand Journal of Psychiatry*, *51,* 32-41

Mazziotta, J., Toga, A., Evans, A., Fox, P., Lancaster, J., Zilles, K. et al. (2001). A probabilistic atlas and reference system for the human brain. *Philosophical Transactions of the Royal Society B: Biological Sciences, 356*, 1293–1322.

Myslobodsky, M.S., Glicksohn, J., Coppola, R. and Weinberger, D.R. (1991). Occipital lobe morphology in normal individuals assessed by magnetic resonance imaging (MRI). *Vision Research*, *31*, 1677–1685.

Narr, K.L., Bilder, R.M., Luders, E., Thompson, P.M., Woods, R.P., Robinson, D. et al. (2007). Asymmetries of cortical shape: Effects of handedness, sex and schizophrenia. *Human Brain Mapping Journal*, *34*, 939–948.

Ono, M., Kubik, S. and Abernathey, C. (1990). *Atlas of the Cerebral Sulci.* New York, US: Thieme Medical.

Patterson, N., Richter, D.J., Gnerre, S., Lander, E.S. and Reich, D. (2006). Genetic evidence for complex speciation of humans and chimpanzees. *Nature*, *441*, 1103–1108.

Previc, F.H. (1991). A general theory concerning the prenatal origins of cerebral lateralization in humans. *Psychological Review, 98*, 299-334.

Rajagopalan, V., Scott, J., Habas, P.A., Kim, K., Corbett-Detig, J., Rousseau, F. et al. (2011). Local Tissue Growth Patterns Underlying Normal Fetal Human Brain Gyrification Quantified In Utero. *Journal of Neuroscience*, *31*, 2878–2887.

Reyes, L.D. and Sherwood, C.C. (2014). Neuroscience and Human Brain Evolution. In *Springer Series in Bio-/Neuroinformatics* (Vol. 3, pp. 11–37). Cham: Springer International Publishing.

Rilling, J.K. and Seligman, R.A. (2002) A quantitative morphometric comparative analysis of the primate temporal lobe. *Journal of Human Evolution. 42*, 505–533

Rilling, J.K., Glasser, M.F., Preuss, T.M., Ma, X., Zhao, T., Hu, X., and Behrens, T.E.J. (2008). The evolution of the arcuate fasciculus revealed with comparative DTI. *Nature Neuroscience*, *11*, 426–428.

Rilling, J.K. (2014). Comparative primate neuroimaging: insights into human brain evolution. *Trends in Cognitive Sciences*, *18*, 46–55.

Rubens, A.B., Mahowald, M.W. and Hutton, J.T. (1976). Asymmetry of the lateral (sylvian) fissures in man. *Neurology*, *26*, 620–624.

Sakai, T., Hirata, S., Fuwa, K., Sugama, K., Kusunoki, K., Makishima, H. et al. (2012). Fetal brain development in chimpanzees. *Current Biology*, *22*, R791–R792.

Samson, D., Apperly, I.A., Chiavarino, C. and Humphreys, G.W. (2004). Left temporoparietal junction is necessary for representing someone else's belief. *Nature Neuroscience*, *7*, 499–500.

Santiesteban, I., Banissy, M.J., Catmur, C. and Bird, G. (2012) Enhancing social ability by stimulating right temporoparietal junction. *Current Biology, 22*, 2274–2277.

Saxe, R. and Kanwisher, N. (2003). People thinking about thinking people: fMRI investigations of theory of mind. *NeuroImage*, *9*, 1835– 1842.

Shapleske, J., Rossell, S.L., Woodruff, P.W. and David, A. S. (1999). The planum temporale: a systematic, quantitative review of its structural, functional and clinical significance. *Brain Research Reviews*, *29*, 26–49.

Shergill, S.S., Brammer, M.J., Williams, S.C., Murray, R.M. and McGuire, P.K. (2000). Mapping auditory hallucinations in schizophrenia using functional magnetic resonance imaging. *Archive of General Psychiatry, 57*, 1033–1038.

Sowell, E.R., Thompson, P.M., Rex, D., Kornsand, D., Tessner, K.D., Jernigan, T.L. and Toga, A. W. (2002). Mapping sulcal pattern asymmetry and local cortical surface gray matter distribution in vivo: maturation in perisylvian cortices. *Cerebral Cortex, 12*, 17–26.

Spocter, M.A., Hopkins, W.D., Garrison, A.R., Bauernfeind, A.L., Stimpson, C.D., Hof, P.R. and Sherwood, C.C. (2010). Wernicke's area homologue in chimpanzees (Pan troglodytes) and its relation to the appearance of modern human language. *Proceedings of the Royal Society B: Biological Sciences*, *277*, 2165–2174.

Smith, S.M., Jenkinson, M., Woolrich, M.W., Beckmann, C.F., Behrens, T.E.J., Johansen-Berg, H. et al. (2004). Advances in functional and structural MR image analysis and implementation as FSL. *NeuroImage*, *23*, Supplement 1, S208-219.

Steinmetz, H., Ebeling, U., Huang, Y.X. and Kahn, T. (1990) Sulcus topography of the parietal opercular region: an anatomic and MR study. *Brain and Language, 38*, 515–533.

Taglialatela, J.P., Dadda, M., and Hopkins, W.D. (2007). Sex differences in asymmetry of the planum parietale in chimpanzees (Pan troglodytes). *Behavioural Brain Research*, *184*, 185–191.

Takao, H., Hayashi, N.,and Ohtomo, K. (2011). White matter asymmetry in healthy individuals: A diffusion tensor imaging study using tract-based spatial statistics. *Neuroscience*, *193*C, 291–299.

de Schotten, M.T., ffytche, D.H., Bizzi, A., Dell'Acqua, F., Allin, M., Walshe, M. et al. (2011). Atlasing location, asymmetry and inter-subject variability of white matter tracts in the human brain with MR diffusion tractography. *NeuroImage*, *54*, 49–59.

Toga, A.W. and Thompson, P.M. (2003). Mapping brain asymmetry. *Nature Reviews Neuroscience, 4*, 37–48.

Tzarouchi, L.C., Astrakas, L.G., Xydis, V., Zikou, A., Kosta, P., Drougia, A. et al. (2009). Age-related grey matter changes in preterm infants: an MRI study. *NeuroImage, 47*, 1148 –1153.

Watkins, K.E., Paus, T., Lerch, J.P., Zijdenbos, A., Collins, D.L., Neelin, P. et al. (2001). Structural asymmetries in the human brain: a voxel-based statistical analysis of 142 MRI scans. *Cerebral Cortex*, *11*, 868–877.

Witelson, S.F. and Kigar, D.L. (1992). Sylvian fissure morphology and asymmetry in men and women: bilateral differences in relation to handedness in men. *Journal Comparative Neurology*, *323*, 326–340.

Xiang, L, Crow, T.J., Hopkins, W.D., Gong, Q. and Roberts, N. (2018). Human torque is not present in chimpanzee brain. *NeuroImage*, *165*, 285-293.

Yeni-Komshian, G.H. and Benson, D.A. (1976). Anatomical study of cerebral asymmetry in the temporal lobe of humans, chimpanzees, and rhesus monkeys. *Science*, *192*, 387–389.

Yakovlev, P. and Rakic, P. (1966). Patterns of decussation of bulbar pyramids and distribution of pyramidal tracts on two sides of the spinal cord. *Transactions of the American Neurological Association*, *91*, 366-367.

Zhao, L., Hietala, J. and Tohka, J. (2009). Shape Analysis of Human Brain Interhemispheric Fissure Bending in MRI. *Medical Image Computing and Computer Assisted Intervention*, *12* (Pt 2), 216–223.

	Humans (*n*: 27)	**Chimpanzees (*n*: 29)**	**Statistical Difference**
Males; Females	*14, 13*	*12, 17*	$\chi 2$ (1, *n: 55*) = 0.446, *p* = 0.504
Average Age (Range)	*30 (19 - 60)*	*20.1 (6- 43)*	*t (53) = 4.093, p < 0.001*

Table 1:
Gender and age profile of the final human and chimpanzee cohort (that were successfully processed through the main pipeline

		Superior Type PAR longer		Inferior Type PDR longer		Symmetric PAR equal		Inverted Type PAR Orientated		Statistical Difference	
Species	Hemisphere		Total		Total		Total		Total	Hemisphere Difference	Species Difference
Humans *n*: 51 hemispheres)	Left	16	38 (74.5%)	6	6 (11.8)	1	2 (3.9%)	1	5 (9.8%)	χ^2 (3, *n*: 51) = 8.601, *p* = 0.035	χ^2 (3, *n:* 88) = 48.06 p < 0.001
	Right	22		0		1		4			
Chimpanzee (*n*: 37 hemispheres)	Left	2	3 (8.1%)	2	3 (8.1%)	0	1 (2.7%)	10	30 (81.0%)	χ^2 (3, *n:* 37) = 2.988, *p* = 0.394, *ns*	
	Right	1		1		1		20			

Table 2:

Bifurcation types of each hemisphere with a bilateral bifurcation point. This is divided by hemisphere and then totaled (with percentage for the species) – Superior Type is most common in humans and Inverted Type for the chimpanzees.

						One Sample *t*-Test			Between Species ANOVA			
Landmark	Axes	Species	Mean AI	SD	N	DF	*T*	*p*	DF	*F*	*p*	α
Anterior Bifurcation (A)	Anterior-Posterior	Human	0.0015	0.0541	27	26	-0.144	0.886	1, 54	1.038	0.313	0.17
		Chimpanzee	0.0218	0.0896	29	28	-1.313	0.2				
	Superior - Inferior	Human	0.0014	0.0327	27	26	0.219	0.828		0.51	0.478	0.108
		Chimpanzee	0.0109	0.0615	29	28	0.954	0.348				
Posterior Bifurcation Point (B)	Anterior-Posterior	Human	**0.0606**	0.0979	27	26	-3.098	0.005**	1, 40	5.716	0.022*	0.645
		Chimpanzee	0.001	0.0367	29	28	-0.117	0.909				
	Superior - Inferior	Human	0.0202	0.0575	27	26	1.757	0.092		1.397	0.244	0.211
		Chimpanzee	0.0024	0.0278	29	28	0.359	0.725				
Termination Point (S1)	Anterior-Posterior	Human	**0.0642**	0.0714	27	26	-4.674	<0.001**	1, 54	0.208	0.65	0.073
		Chimpanzee	**0.0542**	0.0916	29	28	-3.186	0.004**				
	Superior - Inferior	Human	**0.0603**	0.1139	27	26	-2.752	0.011*		6.116	0.017*	0.68
		Chimpanzee	0.0038	0.0454	29	28	-0.446	0.659				

Table 3:

Statistical summary of the positional analysis of each landmark (A, B, S1) AI in both Anterior-Posterior (A-P) and Superior-Inferior (S-I) directions. Positive AI (Asymmetry Index) values over 0.025 indicate that the right is (A-P) more anterior or superior (S-I) on the right hemisphere. *T*- Tests determine how significant the asymmetries are (* is significant, ** is highly significant) and the ANOVA determines if these asymmetries are significantly different between humans and chimpanzees. Other Abbreviations: SD - Standard Deviation; N – Total Sample; DF – Degrees of Freedom; *T* – *T*-statistic; *p* – *p*-value; *F* – *F*-statistic; α – Statistical Power

					One Sample *t*-Test			Between Species ANOVA		
SF Segment	Species	Mean AI	SD	N	DF	*T*	*p*	DF	*F*	*p*
Anterior-Horizontal SF	Human	**-0.191**	0.27	24	23	-3.52	0.002**	1, 35	4.45	**0.042***
	Chimpanzee	-0.017	0.2	14	13	-0.03	0.979			
Vertical SF	Human	**0.383**	0.65	24	23	2.869	0.009**		1.85	0.183
	Chimpanzee	0.104	0.54	14	12	0.85	0.411			
Total SF	Human	-0.058	0.15	24	23	-1.87	0.074		1.29	0.265
	Chimpanzee	0.001	0.16	14	23	0.42	0.682			

Table 4

Statistical summary of the length AI's (Asymmetry Index) in the different segments of the SF. Positive AI (Asymmetry Index) values over 0.025 indicate that the right is (A-P) more anterior or superior (S-I) on the right hemisphere. *T*- Tests determine how significant the asymmetries are (* is significant, ** is highly significant) and the ANOVA determines if these asymmetries are significantly different between humans and chimpanzees. Other Abbreviations: SD - Standard Deviation; N – Total Sample; DF – Degrees of Freedom; *T* – *T*-statistic; *p* – *p*-value; *F* – *F*-statistic.

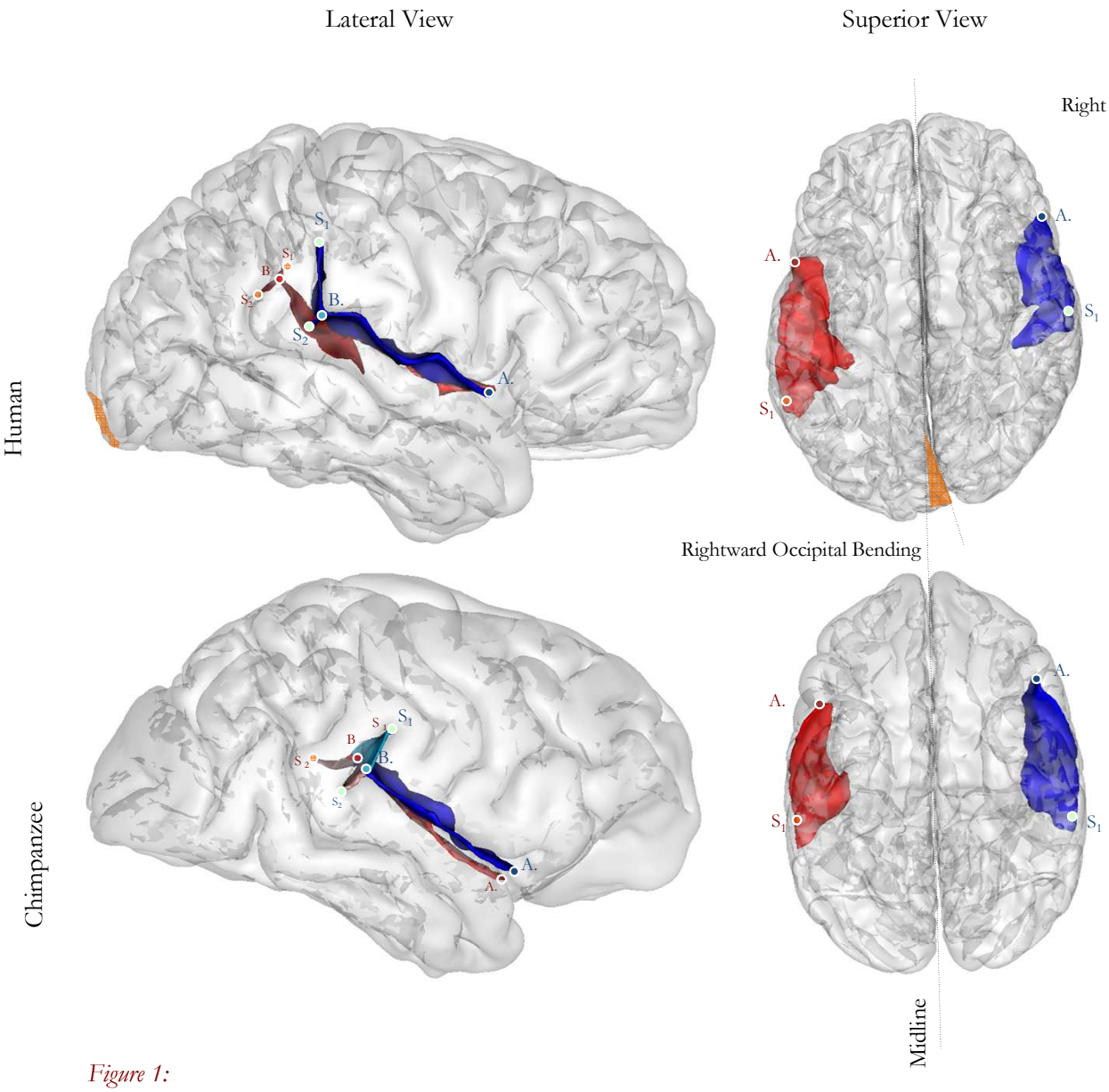

Figure 1:
Example human (above) and chimpanzee (below) brain meshes in both lateral and superior view processed through Freesurfer and BrainVISA with Sylvian Fissure demonstrating the left length asymmetry (red) and the right trajectory asymmetry (blue, more superior and anterior). The landmarks are illustrated: Anterior Bifurcation Point (A), Posterior Bifurcation Point (B), posterior termination point (S_1) and the posterior descending point (S_2). The superior view also demonstrates the rightward occipital bending angle in the human brain using a midline (orange). Brains are not to scale, and are displayed in Native space.

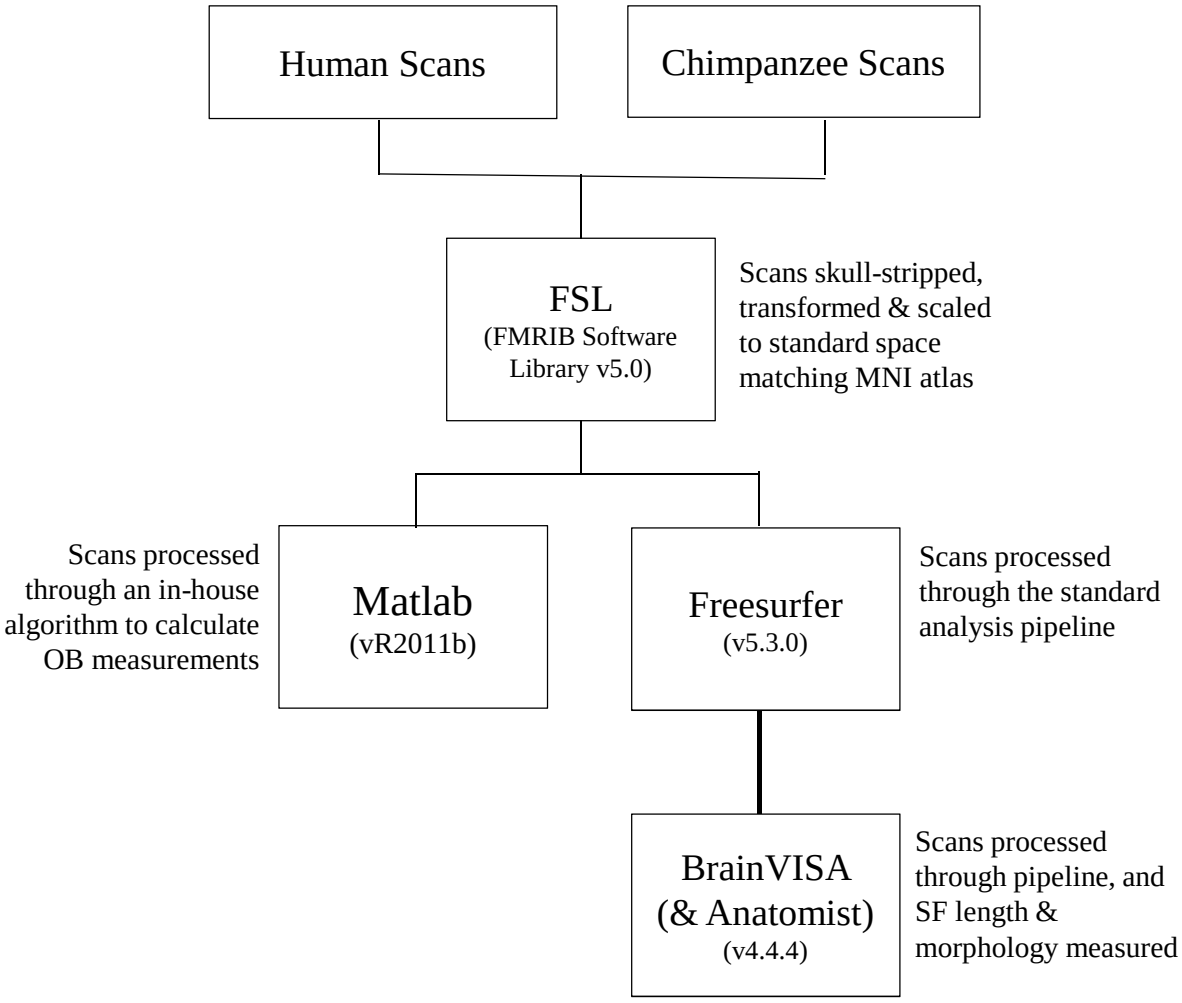

Figure 2:
Overview flow diagram of the data processing steps and software involved in the study analysis for both SF and OB analysis with a small summary. See in text for a more detailed description of each step.

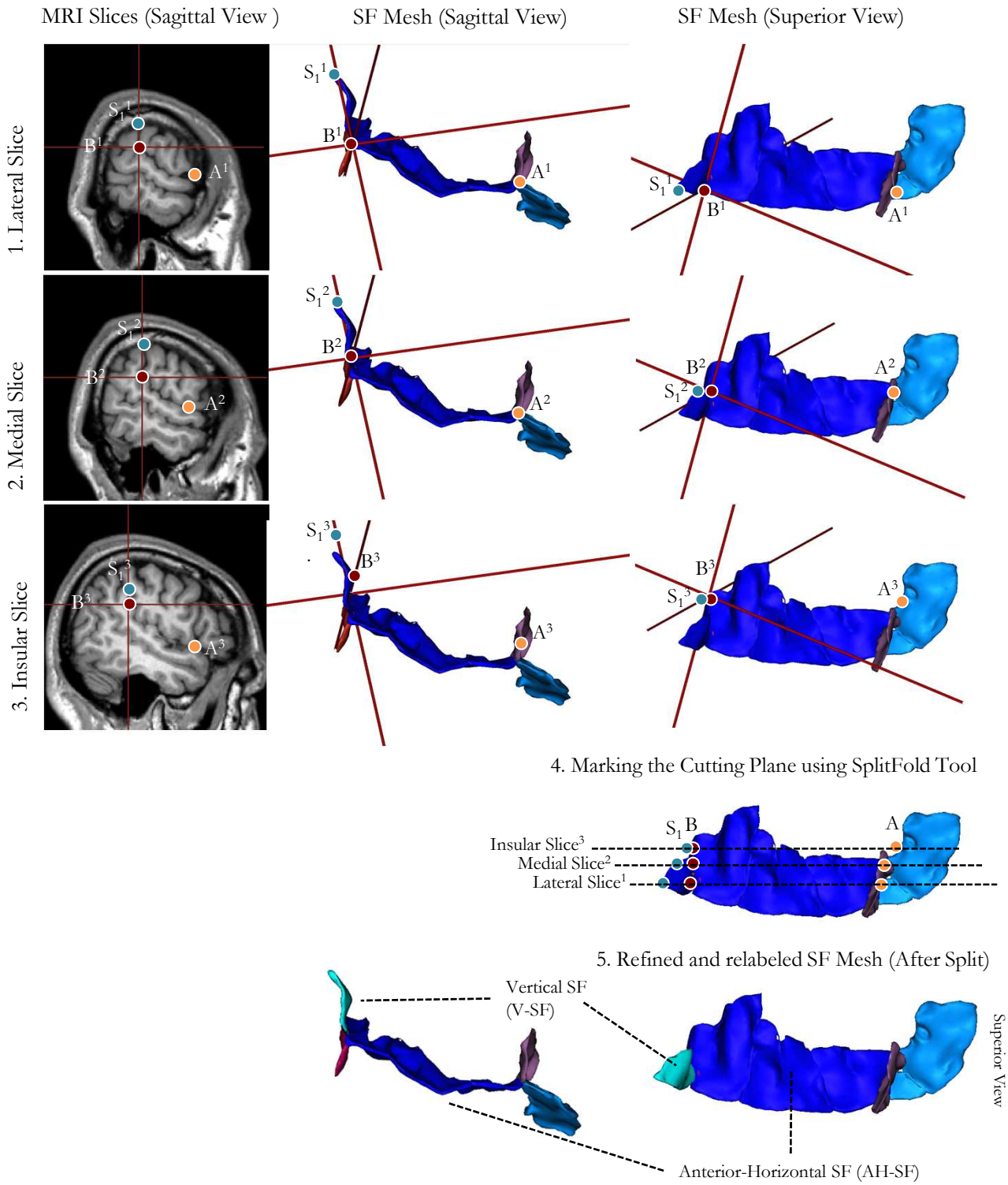

Figure 3:

Stages involved in refining the 3D BrainVISA mesh output to split into the Vertical SF and Anterior-Horizontal SF using Anatomist tools. Landmarks such as the Terminal Point (S_1) and Anterior Bifurcation point (A) and Bifurcation Point (B) are identified in three different MRI slices, from lateral (1), medial (2) and insular (3). These points for (B) is then used to determine the cutting plane using the SplitFold Tool in Anatomist (4) which split the mesh into independently quantifiable cortical folds. Once these are updated, the new mesh between (S_1) and (B) can then be re-labeled into the Vertical SF and Anterior-Horizontal SF and the length can then be measured.

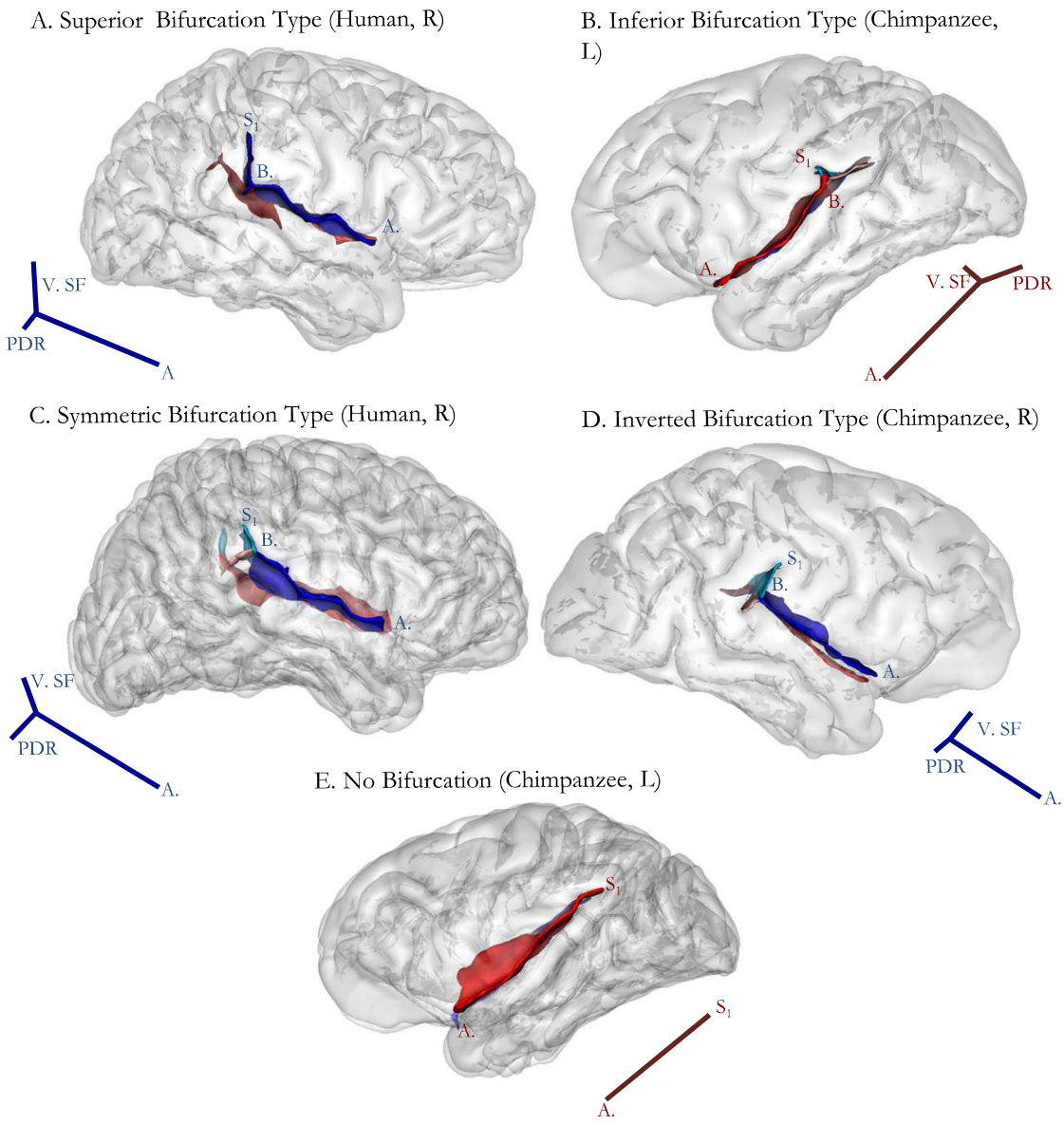

Figure 4:
Examples of the four bifurcation types (A - D), along with an example of a SF without a bifurcation point (E). Species and left (L) versus Right (R) hemisphere specified. Vertical (V.) SF is synonymous to the Posterior Ascending Ramus (PAR) or Planum Parietale, and distinct from the Posterior Descending Ramus (PDR). A. Superior Bifurcation Type: PAR is longer than PDR. B. Inferior Bifurcation Type: PDR is longer than PDR. C. Symmetrical Bifurcation Type: PAR and PDR are similar lengths. D. Inverted Bifurcation Type: PAR is orientated anteriorly rather than posteriorly. E. No bifurcation point. Adapted from Ide *et al.* 1996.

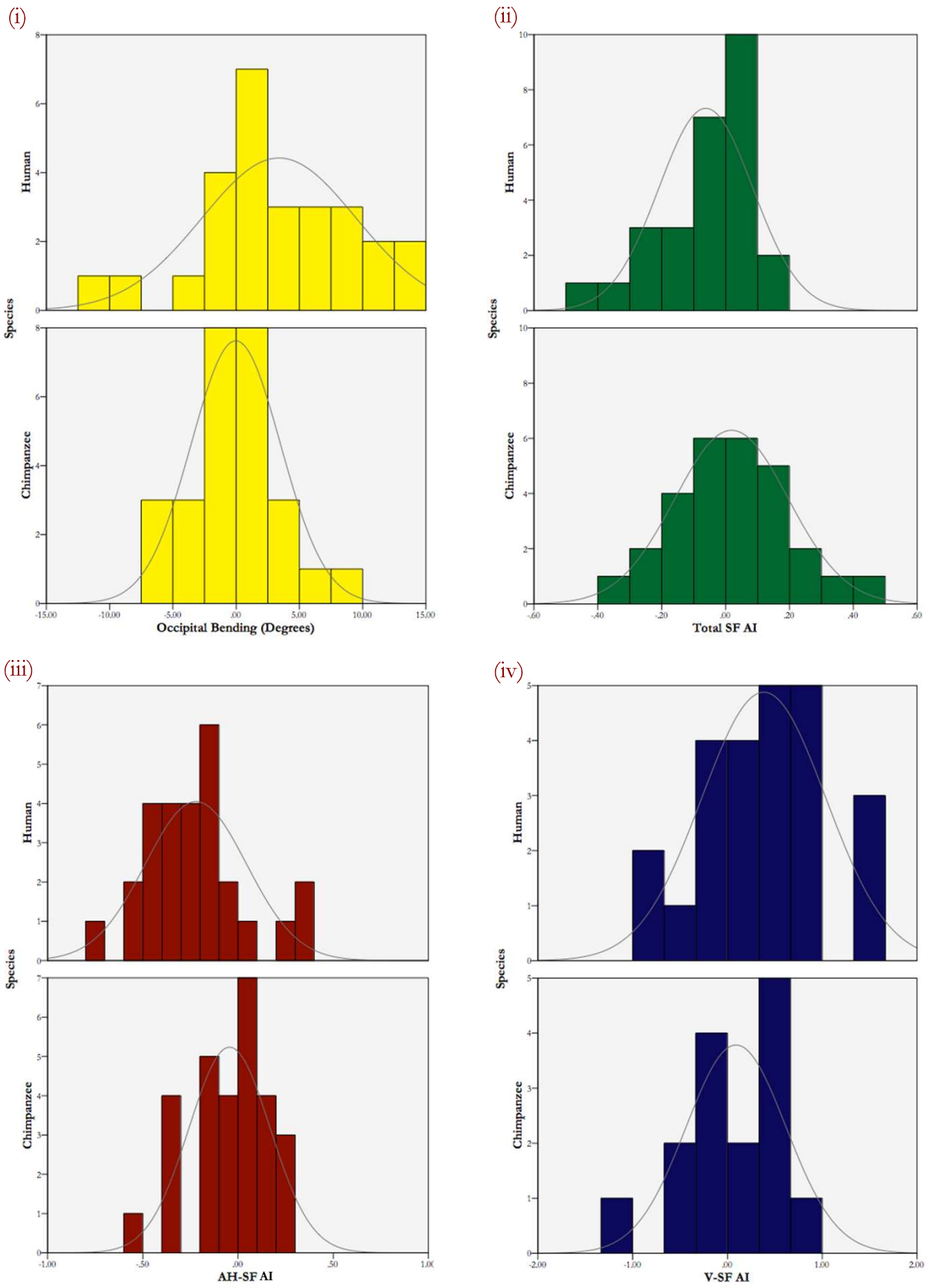

Figure 5: Frequency Distribution Histograms

Histogram figures made from all collected measures for each variable independently. The origin for each histogram are centered, but each is scaled differently. (i) Occipital Bending (Human *n*: 27; Chimpanzee *n*: 27) (ii) Total SF length AI (Human *n*: 27; Chimpanzee *n*: 28) (iii) AH-SF length AI (Human *n*: 27; Chimpanzee *n*: 28) (iv) V-SF length AI (Human *n*: 24; Chimpanzee *n*: 15)

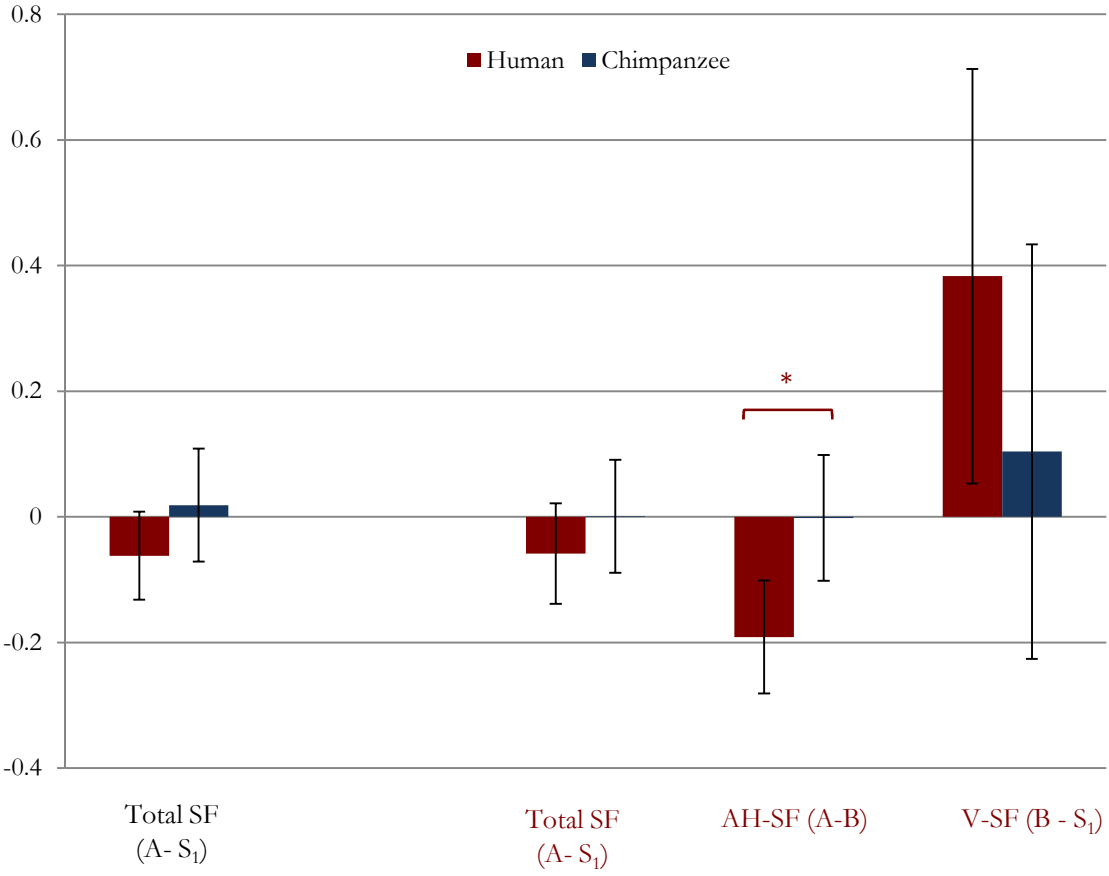

i. **Whole Cohort**
Human *n*: 27
Chimpanzee *n*: 28

ii. **Bifurcation Cohort**
Human *n*: 24
Chimpanzee *n*: 14

Figure 6: Between Group Length AI Comparisons
The Asymmetry Index(AI) of the SF lengths of humans and chimpanzees in (i) the Whole Cohort (humans *n*: 27, chimpanzees *n*: 28) and (ii) further divided in the population with bifurcation points (B) in both hemispheres (human *n*: 24, chimpanzee *n*: 14). In the Total SF ($A - S_1$) in both cohorts, human show a leftward asymmetry in both the whole cohort (Mean AI: -0.062, SD: -0.147) and bifurcation cohort whereas chimpanzees did not (Mean AI: 0.019, SD: 0.178). However, the AI's overall were not significantly different (F (1, 52) = 3.658, p = 0.061, *ns*)

Humans showed the previously reported leftward bias specifically in the AH-SF segment, which was significantly different in chimpanzees (F (1,35) = 4.449, p = 0.042), whereas the V-SF showed the previous established rightward bias in both species, and was not significantly different (F (1, 35) = 1.846, p = 0.183, *ns*). Both of these opposing directions cancelled out in the Total SF, though there was no significant difference between species (F (1, 35) = 1.286, p =0.265, *ns*). Positive AI: Right larger than left. Negative AI: Left larger than right.

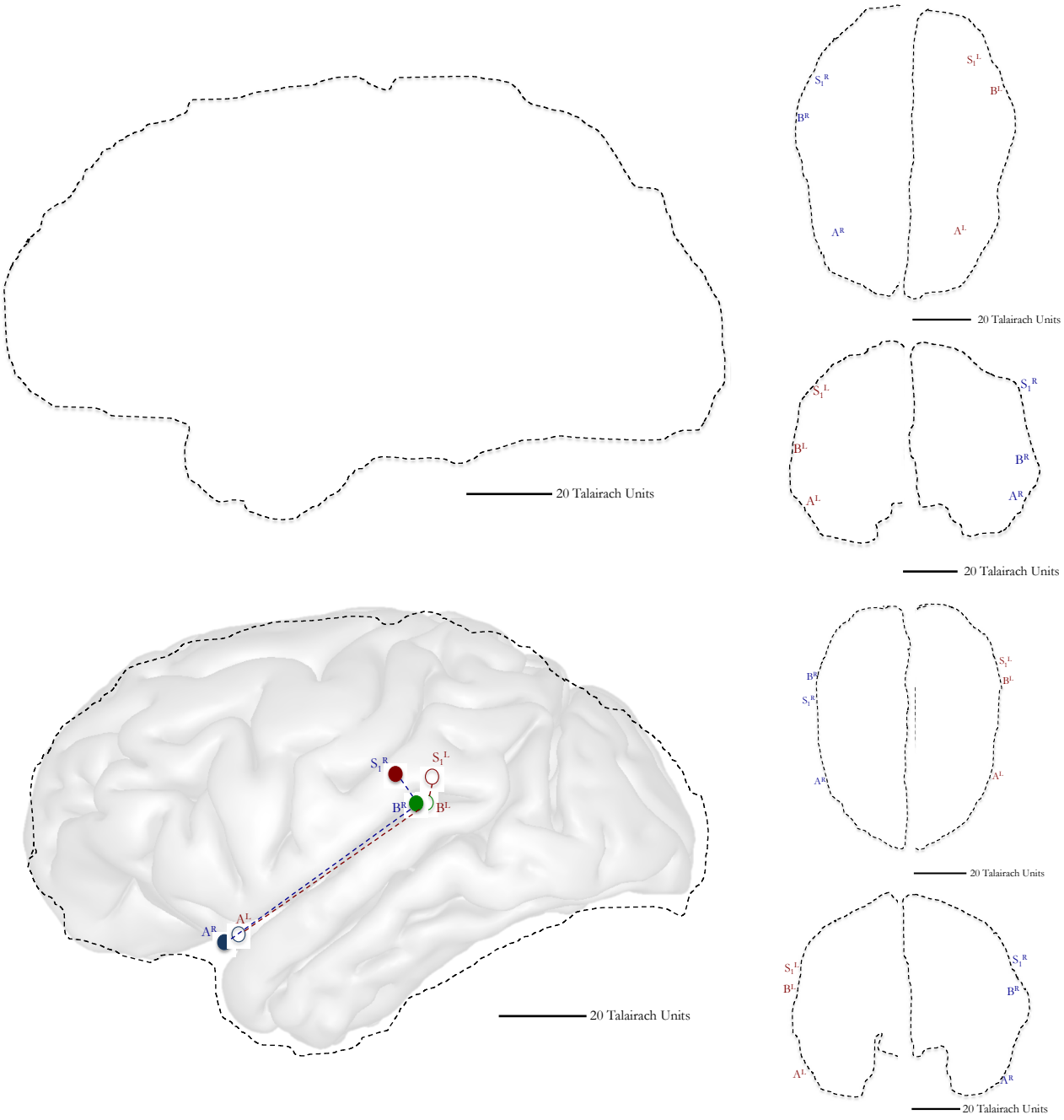

Figure 7: Average trajectories in humans and chimpanzees

Summary diagram with the average trajectories in humans (above) and chimpanzees (below) based on the talairach co-ordinates of the Anterior Bifurcation Point (A), Posterior Bifurcation Point (B) and the Termination Point (S_1) of either the right (^{R}) or left (^{L}) hemisphere. The coordinates are to scale, though the brain outlines are not and are for illustrative purposes only. The more anterior termination of the SF on the right is seen in both SF although only in humans does it terminate more superiorly. The length asymmetries of the anterior-horizontal SF to the left, and the Planum Parietale to the right are also evident in the humans, and absent in the chimpanzees.

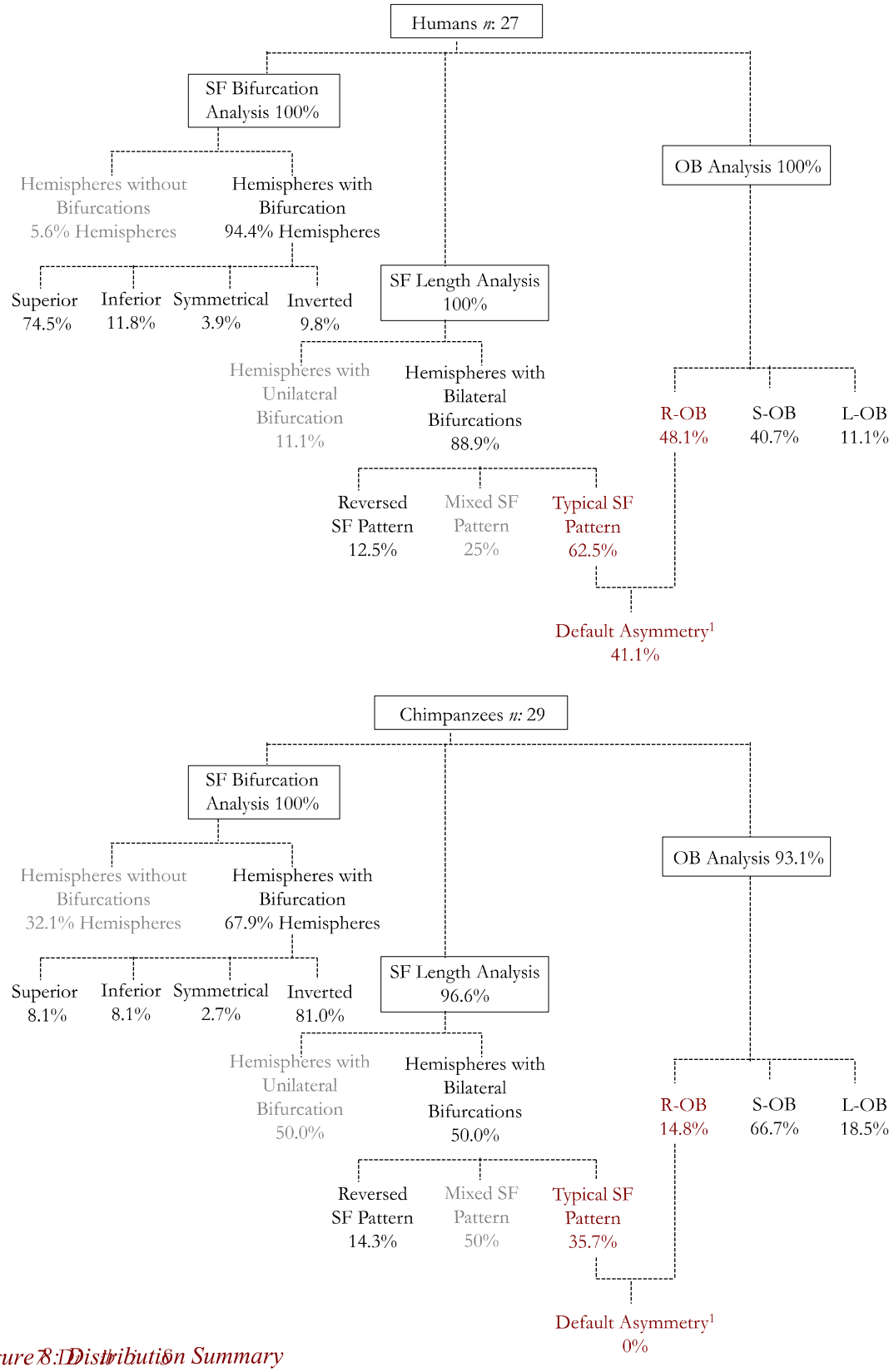

Figure 8: Distribution Summary

Summary of study analysis and distributions for human and chimpanzees. Stage 1 is the percentage of the original sample have been sucessfully processed with the stated analysis. Each subsequent percentage is cumulative of the higher level cohorts. [1] Default Asymmetry distribution is calculated as the percentage of the Typical SF Pattern (Leftward AH-SF, rightward V-SF) cohort with Rightward OB.

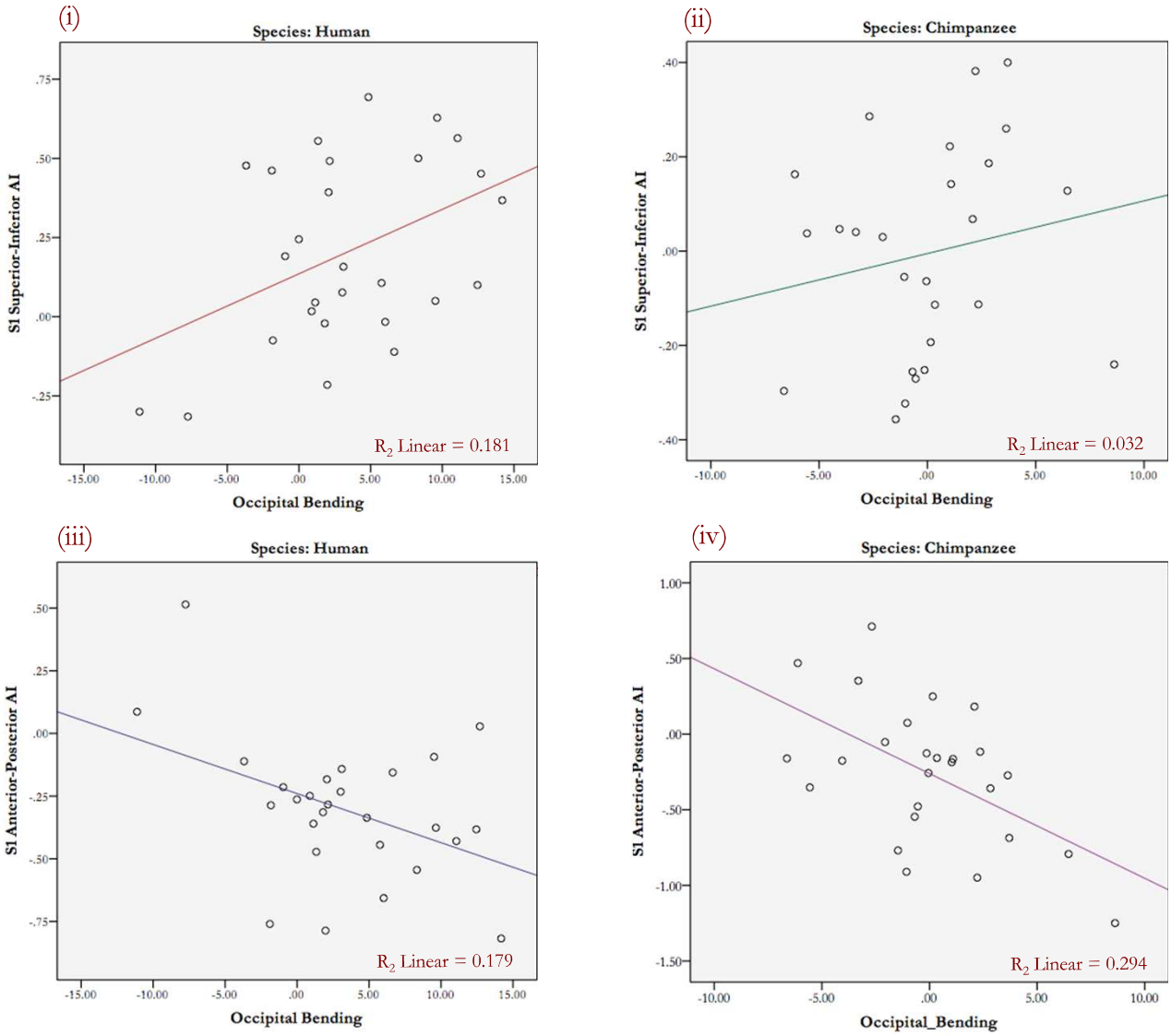

Figure 9: Dispersion Plots of Correlations between Positional Asymmetries and Occipital Bending

Dispersion Plots of the correlational analysis between the positional asymmetry of the Termination Point (S_1) in humans (i, iii) and chimpanzees (ii, iv) independently, in the Superior-Inferior Axis (i, ii) and the Anterior-Posterior Axis (iii, iv). In the human cohort there is a relationship between the position of S1 and OB in both directions (AI on the Superior-Inferior Axis: r: 0.425, p = 0.027, n: 27; AI on the Anterior- Posterior Axis r: -0.423, p = 0.028, n: 27). Chimpanzees have the same relationship in the Anterior-Posterior (r: -0.542, p = 0.004, n: 26) but not Superior-Inferior axis (r: 0.179, p = 0.381, n: 26) though the difference between species did not reach significance (Superior-Inferior Axis AI: Z = 0.93, p = 0.352, two tailed; Anterior-Posterior Axis AI: Z = 0.53, p = 0.60, two tailed).